

OVERVIEW OF RECENT MOUNTAIN-BUILDING EVENTS IN THE BIG BEND REGION, WEST TEXAS AND NORTHERN MEXICO

Joseph I. Satterfield

Department of Physics, Angelo State University, San Angelo, Texas 76909

Richard A. Ashmore

Department of Earth and Space Sciences, Lamar University, Beaumont, Texas 77710
and Department of Biological Sciences, Texas Tech University, Lubbock, Texas 79409

ABSTRACT

The terrain of the Big Bend region, as well as locations of many ore bodies, hot springs, and the Rio Grande River, mostly result from two mountain-building events: Basin and Range extension that continues today, but also Rocky Mountain (or “Laramide”) contraction that ended 50 million years ago. Both events continued for tens of millions of years, producing complex arrangements of folds and faults throughout broad, overlapping zones extending from southern Mexico into Canada. Laramide contraction and Basin and Range extension are caused, at least in part, by changing plate interactions along the western margin of the North American plate. Two compilation maps of the Big Bend region, one showing Laramide structures and one showing Basin and Range structures, summarize current understanding. Panoramic photographs illustrate well-exposed structures in Big Bend National Park. An extensive reference list compiles work on Laramide and Basin and Range structures. Work to date, which includes recent detailed mapping in two small areas, emphasizes several points: a) Laramide structures in the Big Bend region include thick-skinned basement uplifts and coeval thin-skinned thrust belts, b) Map-scale and outcrop-scale folds formed during Basin and Range extension as well as during Laramide contraction, and c) Long-lived fault zones moved repeatedly during Laramide contraction and Basin and Range extension.

Reference:

Satterfield, J.I., and Ashmore, R.A., 2009, Overview of recent mountain-building events in the Big Bend Region, West Texas, and northern Mexico: *Journal of Borderland Studies*, v. 1, 35 p.

INTRODUCTION

In the last 100 million years two continent-wide mountain-building events deformed the Big Bend region of Texas and northern Mexico. First, from about 70 to 50 million years before present (70 – 50 Ma) Rocky Mountain faults and folds shortened and sheared the area. Beginning 30 Ma Basin and Range structures have extended and sheared virtually the same region. Continuing Basin and Range fault movement generates earthquakes today. Records of these events fall mostly within the Texas Lineament, an 80 km-wide belt of northwest-trending faults first active 1400 Ma. The Texas Lineament¹ (boundaries shown as dashed lines on Figure 1) separates these structures from undeformed crust to the northeast (Muehlberger 1980). Mountain-building events and differing erosion rates have produced today's landforms. Rocky Mountain folds and Basin and Range fault blocks capped by thick, resistant limestone, are typically topographic highs today. Hot springs and mercury, silver, and fluorite ore deposits are commonly concentrated in fault zones. The Big Bend region of this paper (Figs. 1, 2) spans 28.9° to 30.3° N latitude; the northern margin is approximately the latitude of US 90 connecting Marathon, Alpine, and Marfa, Texas. The region spans the Rio Grande River from Candelaria to Langry, covering Big Bend National Park and Big Bend Ranch State Park in Texas, Maderas del Carmen Protected Area in Coahuila, and the Santa Elena Canyon Protected Area in Chihuahua. Many well-exposed folds, faults, and rock types described in this paper can be identified on a satellite image of Big Bend National Park and surrounding areas² (Dohrenwend 2002).

The Big Bend region does contain large structures and ore bodies not directly related to Rocky Mountain or Basin and Range mountain building: a) underlying Paleozoic, pre-Rocky Mountain Ouachita/Marathon orogen³ folds and thrust faults exposed in the cores of the Marathon uplift and Solitario (Fig. 1), b) numerous forcefully intruded Tertiary (48 – 17 Ma) plutons that steeply tilted and faulted their margins (more on page 8), c) nine fault-bounded calderas produced by collapse of magma chambers after Tertiary volcanic eruptions (Henry and Price 1985, 1989), c) fluorite and other ore bodies that precipitated from Tertiary pluton-related hydrothermal fluids on or near pluton margins. In northern Coahuila, thirty kilometers southeast of Boquillas (Fig 1) the Aguachile and Pico Etereo fluorspar mining districts contain Tertiary plutons that generated hydrothermal fluids that reacted with limestone, producing fluorite ore bodies in nearby pluton-caused fault breccia zones and along bedding planes (Levinson 1962; Daugherty 1963; McAnulty, et al. 1963; Kesler 1977). The Christmas Mountains fluorspar district, twenty kilometers northeast of Terlingua (Fig. 1), contains fluorite ore bodies along the margins of several plutons that formed in the same way (Daugherty 1981; Henry, et al. 1989). Gold-Lead-Zinc, Molybdenum, manganese, and uranium ore mineralization in prospects within the Solitario are also caused by local Tertiary igneous activity unrelated to Laramide or Basin and Range mountain-building (Henry 1996). In order to describe Rocky Mountain or Basin and Range structures, pluton-caused deformation, and multiple deformation phases, must be distinguished.

¹ A lineament is a linear topographic feature of regional extent caused by an underlying geologic structure, such as a fault zone (Bates and Jackson 1984).

² Available from the Big Bend National Park Visitors Center or <http://www.summitgeology.com/bigbend.html>

³ An orogen is a continent-scale belt of folds and faults that formed in one mountain-building event.

Objectives

The primary objective of this paper is to present a current synthesis and review of geologic data and interpretations concerning Rocky Mountain and Basin and Range mountain-building events in the Big Bend region. This has been achieved by updating and augmenting the most recent summaries (Page, et al. 2008; Henry and Price 1985; Muehlberger and Dickerson 1989; Muehlberger 1989; Maxwell, et al. 1967), by presenting a compilation of geologic structures on two maps (Figs. 1, 2), and by including an extensive reference list. Descriptions from ongoing detailed mapping in two small areas, the Dog Canyon-Dagger Mountain area in northern Sierra del Carmen and in the southeastern Marathon uplift (Figs. 1, 2) complement the work of others. The second objective is to share panoramic photographs of three especially well-exposed and accessible structures produced by Big Bend mountain building (Figs. 3, 4, 5).

The third objective is to describe the two mountain-building events in a way understandable and usable by different disciplines working in the Big Bend region, facilitating interdisciplinary studies. This paper uses basic terms described and pictured in introductory geology texts for non-geology majors. Recently published widely-adopted texts that will help non-geologists understand this paper include Grotzinger, et al. (2006), Reynolds, et al. (2008), and Marshak (2008). Footnotes explain especially significant or unusual jargon. This paper is more focused and more rigorously referenced than geology guidebooks of the Big Bend written for the general public.

Rock types

Two regional maps (Figs. 1, 2) show four generalized geologic map units symbolized by different colors: a) Cretaceous – early Eocene limestone, shale, and sandstone, b) Tertiary igneous rocks, c) Paleozoic sedimentary rocks, and d) Quaternary sediments. Ages and distribution of rock types in the Big Bend region are overall well known (e.g. Maxwell, et al. 1967; McCormick, et al. 1996; King 1937, 1980; Smith 1970). Knowledge of the vertical succession of rock types and of characteristic fossils within the succession provides form surfaces defining folds, documents fault locations and offset amounts, and constrains when structures were active. Cretaceous through early Eocene (~110 – 40 Ma) rocks in and near Sierra del Carmen in the northern part of the area comprise a 1.3 km-thick succession of limestone deposited in shallow marine environments overlain by one kilometer of sandstone and shale deposited in stream and alluvial fan environments (Maxwell, et al. 1967; Moustafa 1988; Lehman 1991). The Cretaceous marine limestone section thickens to four kilometers in the Chihuahua tectonic belt to the southwest (Fig. 1), where it overlies as much as one kilometer of Late Jurassic rock salt, gypsum, anhydrite, and dolomite (DeFord and Haennggi 1970). Tertiary (65.5 – 2.6 Ma) igneous rocks are mafic to felsic lava flows, pyroclastic rocks, and various shapes and sizes of intrusive igneous rocks. Dated igneous rocks mostly range in age from 48 – 17 Ma; igneous activity peaked 38-32 Ma (Henry and McDowell 1986). The oldest known igneous rocks are the 64.2 Ma Red Hills intrusion in the Chinati Mountains (Gilmer, et al. 2003) and Late Cretaceous (99.6 – 65.5 Ma) pyroclastic rocks near northern Big Bend National Park (Hanson, et al. 2007). Most Big Bend ore mineralization is directly related to fluids generated by igneous intrusions of Tertiary age (e.g. Price, et al. 1989).

LARAMIDE MOUNTAIN-BUILDING

Regional Laramide structures in western North America

Rocky Mountain, also termed “Laramide”, structures have a characteristic, but not unique geographic position, age, and style. Best known are about twenty Laramide basement uplifts in the central and southern Rocky Mountains of Wyoming, Utah, Colorado, and New Mexico (Fig. 1B). Typical uplifts are mountain ranges, such as the Front Range uplift in central Colorado, flanked by coeval basins, such as the Denver Basin. Laramide uplifts contain the easternmost folds and faults within the Cordilleran orogen, the belt of folded and faulted rocks that includes the western third of the United States and extends northward through Alaska and southward into Central America (Fig. 1b; e.g. Oldow, et al. 1989; Burchfiel, et al. 1992; Muehlberger 1993). Since, in general, structures in an orogen are oldest in its core, Laramide folds and faults are among the youngest structures in the Cordilleran orogen. Older Cordilleran orogen structures of different styles, including the Mojave-Sonora megashear (e.g. Molina-Garza and Iriondo 2007) are found to the west in Nevada, California, and Mexico (Oldow, et al. 1989).

Laramide-style basement uplifts expose Precambrian, typically older than 1000 Ma, basement brought towards the surface on thrust faults dipping 10 – 35°. Regional compression caused thrust faulting (Lowell 1983; Gries 1983; Clement 1983). Characteristic Laramide “thick-skinned”-style deformation involves ~20 – 30 km-thick blocks bounded by basal, subhorizontal fault detachments in the middle or lower crust (Oldow, et al. 1989). As basement blocks uplifted, subsiding basins on the flanks and within uplifts received sediments from eroding uplifts (Chapin and Cather 1983; Dickinson, et al. 1988). Upright and overturned folds caused by fault movement are common in sedimentary strata above and adjacent to thrust faults (e.g. Mitra and Mount 1998). Most basement uplifts are elongate north-trending blocks, some trend west-northwest and west (Oldow, et al. 1989; Burchfiel, et al. 1992; Miller, et al. 1992). North-trending uplifts, such as the Front Range uplift in central Colorado, commonly include a component of right-lateral strike-slip displacement (e.g. Tetreault, et al. 2008), while west-northwest- and west-trending uplifts display a left-lateral strike-slip component (Tikoff and Maxson 2001). At the same time that Laramide basement blocks were being uplifted, low-angle thrust faults and folds were deforming relatively thin slivers within “thin-skinned” thrust belts in the northern Rocky Mountains of Montana, Canada, and Alaska and in the Chihuahua tectonic belt of Mexico and westernmost Texas (Burchfiel, et al. 1992; Oldow, et al. 1989).

Laramide mountain building and basin formation occurred from ~80 – 40 Ma (e.g. Miller, et al. 1992). A single phase of southwest-northeast shortening may have produced all Laramide structures; different fold and fault orientations could have resulted from coeval movement on pre-existing Paleozoic structures of various orientations (Oldow, et al. 1989; Burchfiel, et al. 1992; Tikoff and Maxson 2001). Others have described conflicting sequences of several Laramide deformation phases affecting the entire region. Bird (1998) inferred N40E⁴ regional shortening from 60 – 55 Ma, followed by N55E shortening from 45 – 40 Ma. Chapin and Cather (1983) interpreted early orogen-wide N70E compression followed by a late phase of N45E compression. Gries (1983) recognized three phases: latest Cretaceous (~70 Ma) east-west

⁴ N40E is a direction read “40° east of north”, a nearly due northeast direction.

compression, then northeast compression, followed by north-south shortening during the Eocene Epoch (56 – 34 Ma).

Laramide Structures in the Big Bend Region

The Big Bend region contains both thick-skinned and thin-skinned structures of Laramide age. However, many continent-wide syntheses of Laramide geology show only thin-skinned thrust belt structures in West Texas and northern Mexico or do not show the Big Bend area at all (Burchfiel, et al. 1992; Miller, et al. 1992; Tikoff and Maxson 2001). Laramide structures span the Texas Lineament but deformation is concentrated along its margins, within the Chihuahua tectonic belt to the southwest and on the flanks of Marathon–El Burro–Peyotes uplift, a Laramide basement uplift on the northeast margin (Fig. 1).

Chihuahua tectonic belt. The Chihuahua tectonic belt is a 140 km-wide zone of generally northwest- and north-northwest-striking thrust faults, strike-slip faults, and folds (Hennings 1994) that extends from Juarez, Chihuahua to south of Monterrey, Nuevo Leon. Figure 1 shows only a small, easternmost portion, which crudely follows the Rio Grande River. Thrust faults in the northeastern part of the belt generally dip southwest, while southwestern thrusts dip northeast. Cross-sections and interpreted seismic sections show ramps dipping up to 80° connecting subhorizontal thrust fault segments (Hennings 1994; Hennings, et al. 1989; Dickerson 1985; Gries and Haenggi 1970). Northeast-striking strike-slip faults are tear faults separating thrust segments (Prothro 1989; Brister 1986). Overturned and upright tight to open folds of several kilometer-wavelength are common. Steep limbs of upright folds in the northeastern margin of the belt dip northeast (Hennings, et al. 1989; Brister 1986). Sierra Grande (Fig. 1) is a prominent ridge and a resistant 120 km-long upright anticline containing evaporate rocks in its core (Gries and Haenggi 1970; Muehlberger 1989). Hennings (1994) calculated that shortening accommodated by folds and thrust faults totalled 20 km (9% shortening) across the entire belt. However, others estimate 50 – 80 km shortening in local areas alone within the northeastern margin (Hennings, et al. 1989). Strike-slip faulting parallel to the tectonic belt has been described at two localities. The Plomosas shear zone in the central Chihuahua tectonic belt is interpreted to be a major northwest-striking left-lateral strike-slip fault (Hennings 1994). In the Indio Mountains, in the eastern margin of the belt, northwest-trending slickenlines⁵ on minor faults suggest a strike-slip-component was distributed on many faults (Rohrbaugh and Andronicos 2000).

The Chihuahua tectonic belt continues far south of the Big Bend region where it changes character. In central Coahuila and Nuevo Leon, thrust faults are located only on the southwest margin of the belt and dip northeast (Charleston, 1981). The La Babia fault (Fig. 1) and the San Marcos fault bound the Chihuahua tectonic belt in Coahuila (Charleston 1981). These lengthy northwest-striking high-angle faults were reactivated several times, most recently in the Pliocene-Quaternary (Chávez-Cabello, et al. 2007). Pre-Laramide late Jurassic movement on the La Babia and San Marcos faults has been interpreted to be left-lateral strike-slip and possibly

⁵ Slickenlines are scrape marks on fault surfaces useful for deducing fault movement directions.

related to the Mojave-Sonora megashear⁶ (Charleston 1981; Molina-Garza and Iriondo 2007). In the Monterrey area the west-trending Sierra Madre Transverse folded belt turns and joins the Chihuahua tectonic belt. The fold and thrust belt continues south of Monterrey as the Sierra Madre folded belt (Charleston, 1981). Central Coahuila and southwestern Mexico also contain Laramide basement uplifts active 46 – 41 Ma (Chávez, et al.2008; Chávez 2008).

Marathon-El Burro-Peyotes uplift. The Marathon uplift and its southern extension, the El Burro-Peyotes uplift comprise an 80 km-wide, several hundred kilometer-long Laramide uplift that continues southwestward into Coahuila and Nuevo Leon (Fig. 1; Jaquot 1978; Charleston, 1981; Dickerson 1985; Lehman 1991, 2002). The uplift exposes Paleozoic rocks as old as Cambrian (542 – 488 Ma) in the Marathon uplift and in two small areas of Sierra del Carmen: north of Dog Canyon (Tauvers and Muehlberger 1988) and east of Boquillas (Carpenter 1997). The Tornillo basin, adjacent to the southwestern flank of the uplift received sediments shed from the rising uplift and is thickest adjacent to the uplift and (Lehman 1986, 1991). Much of the uplift and its margins have not been mapped in detail, so its overall geometry and the amount of shortening on faults and folds within remain poorly constrained.

Several orientations of thrust and strike-slip faults are exposed in northern Sierra del Carmen, Santiago Mountains, and Del Norte Mountains on the southwest flank of the uplift (Poth 1979; Cobb and Poth 1980; Tauvers and Muehlberger 1988; Satterfield and Dyess 2007; Hazzard, et al. 1967). Thrust faults, including the Santiago thrust (Fig. 1), define a narrow, 5 – 10 km-wide belt of faults that dip northeast at 2 – 30° (Satterfield and Dyess 2007; Satterfield, et al. 2007). Atypically, the Maravillas Ridge thrust dips southwest (Cobb and Poth 1980) and the Black Peak thrust steepens from horizontal to 80° (Cobb and Poth 1980). Cross-sections show some thrust faults only slightly offset map-scale fold hinges (Tauvers and Muehlberger 1988; Poth 1979; Cobb and Poth 1980), while in the Dog Canyon-Dagger Mountain area some thrust faults juxtapose dissimilar map units and folds, requiring large thrust displacements (Satterfield and Dyess 2007). Thrust faults have been interpreted to be oblique-slip faults⁷ that include a left-lateral component of displacement, although left-lateral offset or left-lateral fault slip directions on fault surfaces have not been reported (Tauvers and Muehlberger 1988; Lehman 1991). Five short northeast-striking strike-slip faults in the Santiago Mountains are tear faults⁸ coeval with thrusting (Cobb and Poth 1980). Moustafa (1988) described six zones of west-northwest-trending, en echelon⁹ left-lateral strike-slip faults active during Laramide mountain-building. They truncate Laramide map-scale folds whose structural relief decreases towards the faults, implying faulting was synchronous with Laramide folding (Moustafa 1988). Two of twenty-four faults mapped in west-northwest fault zones yielded fault surfaces indicating left-lateral oblique slip (Moustafa 1988). In the Dog Canyon-Dagger Mountain area five fault

⁶ The Mojave-Sonora megashear (Silver and Anderson, 1974) is a late Jurassic (pre-Laramide) strike-slip fault trending from California and Nevada through central Mexico. It accommodated ~800 km left-lateral displacement related to the opening of the Gulf of Mexico (Anderson and Schmidt 1983). Its existence, location, timing, and displacement amount remain controversial (Molina-Garza and Iriondo 2007; Stewart and Crowell 1989).

⁷ Oblique-slip fault movement is a combination of “dip-slip”, vertical movement characteristic of reverse and normal faults, and “strike-slip” or sideways movement, characteristic of strike-slip faults.

⁸ Tear faults are strike-slip faults bounding portions of thrust fault upper plates that move different amounts. They move synchronously with thrusting.

⁹ En echelon faults or folds define a linear zone in which fault or fold orientations are parallel to each other but oblique to the trend of linear zone.

surfaces containing slickenlines indicate dominant normal offset (Satterfield and Dyess 2007; Satterfield, et al., unpublished mapping). Four additional northwest-striking left-lateral strike slip faults in Sierra del Carmen are interpreted to be Laramide structures (Fig. 1; Moustafa 1988).

Asymmetric folds, many termed monoclines¹⁰, are common map-scale and outcrop-scale Laramide structures. Steep fold limbs generally dip southwest in Sierra del Carmen (Fig. 1). Limited data suggest steep limbs dominantly dip northeast on the northeast flank of Marathon-El Burro-Peyotes uplift (Fig. 1; Sonntag and Satterfield, in review). Map- and outcrop-scale folds have consistently north-northwest-striking axial planes and gently plunging fold axes in three widely separated areas in Sierra del Carmen (Satterfield, et al. 2008; Satterfield and Dyess 2007). Eleven map-scale monoclines throughout the Sierra del Carmen trend north-northwest (Moustafa 1988). In the Boquillas Canyon area (Fig. 1) monoclines bend from north-northwest- to northeast-trending, a local deflection interpreted to be caused by basement block rotations between left-lateral strike-slip faults of Laramide age (Maler 1990).

Overtured Laramide folds, also trending north-northwest, have been mapped in widely separated parts of Sierra del Carmen (Satterfield and Dyess 2007; Carpenter 1997; Cobb and Poth 1980; Tauvers and Muehlberger 1989) and in the southeastern Marathon uplift (Sonntag and Satterfield, in review). In the Dog Canyon-Dagger Mountain area map-scale Laramide folds are cross-cut by Laramide thrusts and fold thrusts, establishing that Laramide thrusting occurred within a long interval of folding (Satterfield and Dyess 2007). Figure 3 shows a particularly well-exposed map-scale overturned syncline cross-cut by Dog Canyon.

Structures between the Chihuahua tectonic belt and Sierra del Carmen. The area between the Chihuahua tectonic belt and Sierra del Carmen contains several large and unusual Laramide folds and faults. Many Big Bend area mines are located along Laramide structures in this area; ore mineralization occurred after Laramide deformation ended. Several ranges, including Mariscal Mountain and Sierra San Vicente are gently plunging, north-northwest-trending asymmetric anticlines (Fig 1). Cinnabar (HgS, the major mercury ore) and fluorite (CaF₂) mineralization is concentrated in fold hinges (Daugherty, 1981). Cinnabar ore bodies in the Mariscal anticline hinge are associated with a minor thrust fault and vertical joints (Stenzel 1986; Maxwell, et al. 1967). Laramide folds in Mesa de Anguila southwest of the Terlingua fault (Fig. 2) are gentle, several km-wavelength warps (DeCamp 1985).

The atypically west-trending Fresno-Terlingua monocline (Fig. 1) bounds the Terlingua uplift, a plateau capped by resistant Cretaceous limestone (Erdlac 1990, 1996). Map-scale anticlines and synclines within the Terlingua uplift trend N15W to N50W (Erdlac 1990). The Terlingua monocline contains cinnabar mines of the large Terlingua mining district (Yates and Thompson 1959; Muehlberger 1989; Henry 1996; Sharpe 1980). (Erdlac 1990, 1996) interpreted the monocline and N64E-striking left-lateral strike-slip and oblique-slip faults bounding narrow grabens¹¹ within the Terlingua uplift to be Laramide structures. However,

¹⁰ Monoclines contain one steeply dipping limb between subhorizontal limbs (Davis and Reynolds, 1996); dip directions of steeply dipping limbs of large map-scale monoclines are indicated by arrows on Figure 1.

¹¹ Grabens are elongate valleys down-dropped by recently active normal faults on their margins. Grabens are also termed “bolsons” in the Big Bend area.

Corry, et al. (1990) and Stevens and Stevens (1985, 1989b) argue that the Terlingua uplift and bounding monoclines are post-Laramide structures caused by forceful pluton emplacement. Such structures, not related to regional mountain-building events, are common throughout the Big Bend. Well-documented examples of domes caused by forceful pluton emplacement in or near the Terlingua uplift include the Solitario dome, which crosscuts the north end of the Terlingua uplift (Fig. 1; Henry and Muehlberger 1996), Black Mesa dome (Henry and Erdlac 1996), Packsaddle Mountain (Moon 1953), Paisano Peak laccolith (Henry, et al. 1989), Adobe Walls dome (Henry, et al. 1989), and Christmas Mountains dome (Henry and Price 1989). Pluton-caused structures are scattered throughout the Big Bend region. Other structures produced by exposed Tertiary plutons mapped in detail include Aguachile Mountain (McAnulty, et al. 1963) and La Cueva dome (Daugherty 1963) in the Pico Etereo fluorspar district, and the McKinney Hills laccolith in Sierra del Carmen (Zimmerman 2005; Martin 2007).

The Chalk Draw and Tascotal Mesa faults (Fig. 1) are well documented representatives of at least four extremely long, west-trending faults that moved in the Paleozoic Era (542 – 251 Ma) and later accommodated left-lateral displacement during Laramide mountain-building (Dickerson 1980, 1981; Muehlberger and Dickerson 1989; Stevens and Stevens 1989b). The Chalk Draw fault is the southern boundary of the Paleozoic Marfa basin (Dickerson 1980) and lines up with the Paleozoic Carta Valley fault zone 100 kilometers to the east (Ewing 1985). Silver-lead-zinc mineralization in the Shafter area is localized along the Chalk Draw fault (Dickerson 1980; Head 2002). The eastern Chalk Draw fault may cross-cut thrust faults in Sierra del Carmen (Dickerson 1980).

Deformation phases. As in the rest of the Laramide orogen, one phase of east-northeast compression may have produced most Laramide structures. Tectonic stylolite orientations indicate N58E compression throughout the Big Bend region (Erdlac 1994). Calcite twinning petrofabric analyses in Sierra del Carmen indicate consistent N70E compression (Moustafa, 1988). Geologic maps of several areas in Sierra del Carmen and Santiago Mountains show a single phase of Laramide folding and faulting (Tauvers and Muehlberger 1988; Toelle 1981; Satterfield and Dyess 2007; Satterfield, et al. 2008; Poth 1979; Cobb and Poth 1980; Moustafa 1988; Hazzard, et al. 1967). Detailed mapping distinguished Laramide folds and faults, designated second deformation phase (D_2) structures, from older syn-sedimentary¹² folds (D_1 structures) and younger Basin and Range faults and folds (D_3 structures).

A second, earlier Laramide deformation phase of northeast shortening has been recognized in several widely scattered areas. In the Malone Mountains within the Chihuahua tectonic belt northwest-trending folds are refolded by north-trending folds (Berge 1984). In the Indio Mountains within the Chihuahua tectonic belt, slickenlines on Laramide fault surfaces group in two sets, one indicating northeast compression and one indicating east-northeast compression (Price, et al. 1985, Prothro 1989). In the southeastern Marathon uplift the map-scale northwest-trending monocline shown on Figure 1 may be refolded by north-northwest-trending open and overturned folds (Sonntag and Satterfield, in review). This early Laramide phase locally present in the Big Bend region may correlate with the first Laramide phase in the northern Rocky Mountains described by Bird (1998).

¹² Syn-sedimentary folds and faults form during or shortly after sediments are deposited and before sediments are cemented or compacted into sedimentary rocks.

Timing. Laramide deformation in the Big Bend region began by at least ~70 Ma and continued until ~50 Ma, during the same time when Laramide structures were active in Colorado and adjacent states. Wilson (1970) stated that most syn-mountain building sediments were deposited in the early or middle Eocene Epoch (~56 to ~40 Ma). Lehman (2002b, 1991) described three times of deformation and synorogenic sedimentation in the Tornillo basin: 70-65 Ma (Late Cretaceous Period), 57-54 Ma (early Eocene Epoch of the Tertiary Period), and 54-51 Ma (prior to middle Eocene). Maxwell, et al. (1967) interpreted six regional unconformities ranging in age from late Early Cretaceous (~100 Ma) through the end of the Middle Eocene (~47 Ma) to have been triggered by regional uplift. One Laramide fold deforming Late Cretaceous Aguja Formation in the Tornillo basin was eroded and overlain by unfolded Middle Eocene Canoe Formation, which constrains Laramide folding in this area to be no older than 70 Ma, the age of uppermost Aguja Formation, and no younger than 47 Ma, the age of the lowermost Canoe Formation (Lehman 2004). Erdlac (1990) and Erdlac and Henry (1994) interpreted the Terlingua monocline to have formed after 68 Ma, the age of the youngest unit folded, and before 50 Ma, the inferred age of an untilted conglomerate unconformably overlying the monocline. However, Stevens and Stevens (1985, 1989b) and Corry, et al. (1994) argue the Terlingua monocline formed by forceful magma intrusion after ~20 Ma because one prominent northeast-trending graben they interpret to predate the Terlingua uplift appears to have formed ~20 Ma.

Similarly broad timing constraints are provided by cross-cutting relations between structures and plutons. Dikes and sills in the Dog Canyon-Dagger Mountain area cross-cut a Laramide thrust fault and fold (Satterfield, et al. 2007), constraining Laramide deformation to be older than 31 – 32 Ma, the age of correlative nearby dated plutons. Apparently folded sills in limbs and hinges of the Mariscal Mountain and adjacent Cow Heaven anticlines (Maxwell, et al. 1967; Bumgardner 1976) are dated at 37 Ma ($^{40}\text{Ar}/^{39}\text{Ar}$ technique on plagioclase feldspar; Harlan, et al. 1995) and 46.5 Ma (U-Pb technique on zircon; Miggins, et al. 2006), ostensibly constraining folding of anticlines to have occurred after 46.5 Ma. However paleomagnetic studies of two Mariscal Mountain sills indicate they were not tilted after crystallization, indicating that folding occurred before 46.5 Ma and/or 37 Ma (Harlan, et al. 1995). Isotopic dates of igneous and metamorphic rocks that formed during Laramide mountain building provide additional times of deformation. Metamorphic minerals that formed during Laramide deformation from nine samples within the Chihuahua tectonic belt 55 km south of Juarez, Mexico yielded ages of metamorphism from 92.5 Ma to 77.7 Ma (K-Ar technique on mica; Denison, et al. 1970). Dikes dated at 37 – 32 Ma are dominantly subvertical and east-northeast-striking, indicating east-northeast Laramide compression during this time interval, although the dikes indicating compression are not folded (Price and Henry 1984, 1988).

Interpretations from Big Bend Laramide Structures. Many, perhaps most asymmetric map-scale folds shown on Figure 1 can be interpreted to be fault propagation folds caused by underlying “blind” thrust faults¹³ (e.g. Mitra and Mount 1998; Davis and Reynolds 1996). Several arguments support this interpretation. Subsurface data from drilling and seismic profiling has shown that fault propagation folds are common in classic Laramide uplifts in Colorado and surrounding states (e.g. Mitra and Mount 1998). Big Bend folds are of the same style and orientation as ideal fault propagation folds (Mitra and Mount 1998). Laramide thrust faults and adjacent related folds are exposed in Sierra del Carmen, Santiago Mountains (Cobb

¹³ A blind fault does not cross-cut the Earth’s surface.

and Poth 1980; Carpenter 1997; Satterfield and Dyess 2007), and the Terlingua monocline (Erdlac, 2002). The unusual west-trending orientation of the Terlingua monocline (Fig. 1) has been explained by considering it to be a fault propagation fold above a reactivated Paleozoic west-striking fault parallel to the Tascotal Mesa and Chalk Draw faults (Dickerson 1981; Erdlac 1990, 2002). In Sierra del Carmen widespread north-northwest-trending monoclines have been interpreted to indirectly result from N70W shortening on west-northwest-striking blind thrust faults (Moustafa 1988). Alternatively, Sierra del Carmen monoclines could form above north-northwest-trending blind thrust faults along the southwest margin of the Marathon-El Burro-Peyotes uplift (Moustafa 1991).

Differences in rock types and thicknesses can explain why thin-skinned thrust-faults and folds in the Chihuahua tectonic belt and thick-skinned folds and faults in Sierra del Carmen and eastward formed at the same time from the same forces. Lower Chihuahua thrust belt thrust faults become subhorizontal within weak Jurassic evaporite beds not deposited elsewhere in the Big Bend region (Gries and Haenggi 1970; Hennings 1994). Also the lower Cretaceous section in the Chihuahua tectonic belt is ten times thicker than in Sierra del Carmen, which provided more possible detachment levels for thrusting and thicker intervals of thin-bedded, more easily deformed strata. The abrupt thickness increase occurs at inferred syn-depositional, pre-Laramide normal faults at the eastern margin of the tectonic belt (Hennings, et al. 1989).

Laramide structures throughout the Big Bend region have been interpreted to comprise one or several transpressional¹⁴ fault zones (Dickerson 1985; Tauvers and Muehlberger 1989; Cobb and Poth 1980). Coeval left-lateral strike-slip faults and thrust faults shown on Figure 1 support this interpretation. East-northeast compression is interpreted to reactivate Paleozoic west-striking faults as left-lateral strike-slip and oblique-slip faults. Big Bend Laramide structures have been interpreted to link together into flower structures, characteristic arrangements of transpressional or transtensional¹⁵ fault zones where faults steepen and join a master strike-slip fault at depth (e.g. Wilcox, et al. 1973). Thrust faults that dip in opposing directions, small-displacements on thrust faults, and en echelon folds are characteristic of flower structures support the flower structure model (Dickerson 1985).

Causes of Laramide Mountain-building

Long-lived subduction at the convergent plate boundary between the North American Plate and several plates to the west produced the Cordilleran orogen (e.g. Dickerson and Snyder 1978; Burchfiel, et al. 1992). Contrasting plate-tectonic models seek to explain the cause of Laramide mountain building (e.g. English and Johnston, 2004). In the orogenic float model (Oldow, et al. 1989; Oldow, et al. 1990; Burchfiel, et al. 1992; Lowell 1983) a major subhorizontal thrust detachment in the middle to lower crust connected thrust faults bounding Laramide uplifts to basal detachments of thrust belts to the west and to basal thrust faults in the accretionary prism at the plate boundary itself. This arrangement allowed plate convergence forces to be transferred far inland. The flat-slab subduction model (Dickinson and Snyder 1978; Bird 1998) proposed that the dip angle of the subducted plate decreased to become nearly

¹⁴ Transpression is a combination of reverse and strike-slip fault displacement in a fault zone or region.

¹⁵ Transtension is a combination of normal and strike-slip fault displacement.

subhorizontal during Laramide deformation, shutting off volcanic arc magma sources. Shearing of the subhorizontal plate against the bottom of the North American plate created Laramide folds and faults. In contrast, the “hit and run” collision model (Maxson and Tikoff 1996; Tikoff and Maxson 2001) proposed that collision of Baja British Columbia, a large far-travelled block, with North America generated compression responsible for Laramide structures. After collision, the block was displaced northward on strike-slip faults from the latitude of Baja California to its present position in British Columbia.

BASIN AND RANGE MOUNTAIN-BUILDING

Regional Basin and Range structures in western North America

The Basin and Range province is a vast region of alternating elongate, fault-bounded mountain ranges and valleys caused by recent extension that continues today in many parts. The province extends from the United States – Canadian border into southern Mexico and is 800 km wide in many places (Dickinson 2006; Stewart 1998; Henry and Aranda-Gomez 1992). It covers a large part of the Cordilleran orogen, including part of the Laramide orogen (Fig. 2b). Irregular boundaries terminate at large, relatively unfaulted blocks including the Sierra Nevada batholith, the Colorado Plateau, and Sierra Madre Occidental. The Basin and Range Province is topographically high because it overlies thin mantle lithosphere and an elevated asthenosphere (e.g. Burchfiel 1992). The Big Bend region falls mostly within the eastern margin of the Basin and Range province in the southern Rio Grande Rift sub-province (Fig. 2b; Stewart 1998; Muehlberger, et al. 1978; Dickerson and Muehlberger 1994; Dickinson 2006; Oldow, et al. 1989).

Normal faults in fault block mountains. Mountain ranges and broad valleys trend north or north-northeast throughout the Great Basin of Nevada and western Utah, the most typical region of the Basin and Range (Stewart 1980, 1998). Spacing of ranges and basins averages 30 km. Mountain crest elevations range from 1500 m to almost 4000 m, while valley floors are 1200 – 2000 m elevation. Recently active range-bounding faults produce steep range fronts (Stewart 1980, 1998; Edwards and Batson 1990). Range front faults are typically steep, 60°-dipping (Stewart 1980) normal faults that curve to become low-angle normal faults at depth (Robison 1983). Some range front faults record recent episodes of right-oblique slip (Caskey, et al. 1996). Middle and late Cenozoic rocks over large, 50 – 200 km-wide areas comprising many ranges share a consistent tilt direction (Stewart 1998).

Seismic sections and data from oil wells show basins contain 2 – 4.5 km of volcanic and sedimentary rocks (Oldow 1992) in asymmetric half-grabens¹⁶. Alluvial fan, stream, and lake deposits that filled the subsiding basin thicken and dip towards the master fault, indicating sediments accumulated during protracted fault movement. The overall amount of extension across fault block mountains of the Great Basin is small, 10-30% (Wernicke 1992; Oldow, et al. 1989; Zoback, et al. 1981).

¹⁶ Half-grabens are basins in which sediments thicken towards a large-displacement normal fault on one flank.

Low-angle normal faults in areas of extreme extension. Around twenty-five small, several-km-wide areas of extreme extension define two broad belts within the Basin and Range: a north-trending belt, extending from southern British Columbia through northeastern Nevada and northwestern Utah, and a northwest-trending belt in Arizona and northern Sonora (Oldow, et al. 1989). These zones of extension, termed metamorphic core complexes (e.g. Armstrong 1984) expose a low-angle normal fault, initially dipping $<30^\circ$ and metamorphic rocks that formed in the middle crust. Metamorphic rocks in the lower plate, which are partly incorporated in the upper plate by large-displacement fault movement, include a thin, one to two kilometer-thick shear zone formed by normal fault movement at mid-crustal depths overprinted on older metamorphic structures that formed during Cordilleran contraction (Oldow, et al. 1989; Burchfiel, et al. 1992). Lower-plate metamorphic rocks may also contain intrusive igneous and metamorphic rocks indicating extensive partial melting in the crust synchronous with extension (Kruckenberg, et al. 2008). Upper-plate Tertiary sedimentary and volcanic rocks exposed on the flanks of typical metamorphic core complexes are steeply tilted by several generations of high-angle normal faults synchronous with deep ductile fault movement. Upper plates in the northern belt moved west and northwest. Most upper plates in the southern belt moved northeast or southwest (Oldow, et al. 1989; Dickinson 2006). Low-angle faults containing km-scale grooves produced during fault movement have been warped into broad domes caused by uplift triggered by lower-plate unloading (Wernicke, 1992).

Strike-slip and normal faults in the Walker Lane belt. The Walker Lane belt (Fig. 2b) is a northwest-trending, 100 km-wide transtensional fault zone in western Nevada, on the western margin of the Basin and Range. Its eastern boundary is marked by an abrupt change from north-northeast-trending fault block mountains to fault block mountains of varied orientations; its western boundary is the Sierra Nevada batholith (Hardyman and Oldow 1991; Stewart 1998). Fault types include steep normal faults, low-angle normal faults, right-lateral strike-slip faults, and left-lateral strike-slip faults (Stewart 1988). Northwest-striking right-lateral strike-slip faults are the most prominent structures of the central Walker Lane (Hardyman and Oldow 1991). North-northwest-striking and north-northeast-striking right oblique faults are also mapped. Left-stepping en echelon right-lateral strike-slip faults accommodate 60 – 75 km offset (Oldow 1992). Most gold-silver mineralization in the Walker Lane occurs along northwest-trending strike-slip faults, possibly because they are reactivating faults of the Pine Nut fault system, a Jurassic – Cretaceous strike-slip fault zone, (Hardyman and Oldow 1991).

Three styles of low-angle normal faults are present. “Domino-” or “Yerington-” style low-angle normal faults greatly extended Tertiary and pre-Tertiary rocks in the Yerington and Hall mining districts on the margins of the Walker Lane. In the Yerington porphyry copper mining district, listric¹⁷ normal faults crosscut Tertiary and pre-Tertiary rocks and older generations of listric normal faults. Beds in upper plates are tilted $75 - 90^\circ$ west while older, originally steep normal faults are now subhorizontal. Comparison with pre-extension cross-sections documents 200% extension (Proffett 1977; Proffett and Dilles 1984; Oldow, et al. 1989). A second style of subhorizontal normal fault produces “transtensional nappes” (Hardyman and Oldow 1991) containing tilted Tertiary volcanic rocks and listric normal faults that sole into basal subhorizontal detachment above untilted, non-metamorphosed pre-Tertiary rocks. Transtensional nappes are linked to coeval strike-slip faults (Hardyman and Oldow 1991).

¹⁷ Listric fault surfaces are scoop-shaped and flatten with depth.

One metamorphic core complex within the Walker Lane belt, the Silver Peak Lone Mountain extensional complex (Oldow 1992; Oldow, et al. 1994), contains a third style of low angle normal faults.

The Silver Peak-Lone Mountain extensional complex transferred displacements between the right-lateral strike-slip Southeast California shear zone and the Walker Lane (Oldow, et al. 1994). East-northeast faults in the central Walker Lane, which originated as jogs in the late Precambrian continental margin, are part of curved fault networks that transfer displacements through the central Walker Lane and into the northern Walker Lane (Oldow 1992). However, Stewart (1988, 1998) interprets east-northeast fault segments to be reactivated Mesozoic strike-slip faults that cross-cut major northwest-trending strike-slip faults. Together the Southeast California shear zone and the Walker Lane accommodate ~25% of the displacement between the Pacific Plate and the North American Plate (Oldow, et al. 2003). Displacements within the Walker Lane are partitioned between coeval strike-slip and normal faults, which requires an underlying basal detachment in the lower crust or upper mantle (Oldow 1992).

Phases and timing of deformation. In general, three deformation phases are recognized throughout the Basin and Range province. Only the most recent phase produced modern Basin and Range topography in the Great Basin. The first, pre-Basin and Range phase produced metamorphic core complexes of different ages formed by extension in different directions. Northern belt metamorphic core complexes range in age from 61 to 20 Ma (Oldow, et al. 1989; Dickinson 2006; Kruckenberg, et al. 2008). Their low-angle normal fault surfaces indicate N60W extension in the western Great Basin (Oldow, et al. 1989). Southern belt metamorphic core complexes are younger, from 20 – 18 Ma, and indicate northeast extension (Oldow, et al. 1989; Dickinson 2006). Within the same interval, from 29 – 18 Ma, east-trending half-grabens opened by north-south extension in the Walker Lane (Hardyman and Oldow 1991). A second phase produced faults, an extensive Great Basin rift zone, and dike swarms indicating N68E extension throughout the Basin and Range province (Zoback and Thompson 1978; Oldow 1992). East-northeast extension occurred from 20 – 10 Ma (Zoback, et al. 1981; Hardyman and Oldow 1991). The third, “classical Basin and Range” phase is uplifting and extending Basin and Range fault block mountains and producing transtension in the Walker Lane. Present-day extension directions interpreted from fault slip analysis, earthquake data, and global positioning system (GPS) measurements consistently trend N55W throughout most of the Basin and Range, but shift to N80E in the western Walker Lane (Oldow 2003; Zoback 1989). The oldest fault-controlled basins related to modern topography are 11 – 13 Ma old (Stewart 1980; Zoback, et al. 1981). Low-angle normal faulting on the Silver Peak-Lone Mountain extensional complex related to Walker Lane transtension occurred 11 – 6 Ma (Oldow, et al. 1994). Faults active in the Quaternary Period bound at least one flank of most ranges throughout the Great Basin (U.S. Geological Survey and Nevada Bureau of Mines and Geology 2006; Wallace 1984; Stewart 1980). Historical fault scarps and earthquake epicenters define three belts where faults are most active today: the Walker Lane belt on the western margin of the Basin and Range province, the Central Nevada Seismic Belt, and the Wasatch fault zone in southeastern Idaho and central Utah (Wallace 1984; Oldow, et al. 2001).

Basin and Range structures in the Big Bend region

Basin and range structures in northwest and north-northwest-trending fault block mountains in the Big Bend region primarily consist of several orientations of high-angle faults. Coeval map-scale and outcrop-scale folds are adjacent to faults. Elevations range from over 2500 m in Sierra del Carmen and the Chisos Mountains to less than 500 m along the Rio Grande River.

Faults. Four sets of fault orientations and types are shown on Figure 2: a) north-northwest-striking normal faults, b) northwest-striking normal faults, c) west-striking regional strike-slip fault zones, and d) northwest-striking strike-slip faults. A fifth set, northeast-striking normal faults, have only been described north of the Big Bend area. North-northwest- and northwest-trending normal faults bound five large grabens (Fig. 2; Muehlberger and Dickerson 1989) and are the most common fault types within and among the basins. Large named basins are slightly asymmetric grabens bounded by master faults that accommodated 200 – 1600 m normal offset (Carpenter 1997; Henry 1998a; Dickerson and Muehlberger 1994; St John 1966). Graben-bounding faults form straight, abrupt range fronts, including the 500 m-high Terlingua fault escarpment at the mouth of Santa Elena Canyon which bounds the Castelon graben (Fig. 2) and the 1200 m-high escarpment on the Del Carmen fault (minimum 1600 m displacement) south of the Rio Grande River (Fig. 2; Carpenter 1997; MacLeod 2003). Individual grabens trend north-northwest or northwest (e.g. Dickerson and Muehlberger 1994). Fault surfaces on some or perhaps many north-northwest-trending faults record different times of strike-slip and normal fault movement (Maler 1990; Hentz and Henry 1989; Stevens and Stevens 1989). Strata within basins dip less than 10° towards the master faults (Henry 1998a; Henry and Erdlac 1996). North-northwest- and northwest-striking faults dip 60 – 90° (Moustafa 1988; Maler 1990; Henry 1998a; Dickerson and Muehlberger 1994; Henry and Erdlac 1996; Stevens and Stevens 1989; Satterfield and Dyess 2007). Faults generally do not extend into large areas of intrusive igneous rocks such as the Chisos Mountains and the Solitario (Fig. 2; Henry 1998a). The Rio Grande River in New Mexico and the Big Bend region mostly occupies structurally and topographically low grabens bounded by northwest- and north-northwest normal faults (Fig. 2; Muehlberger and Dickerson 1989; Henry 1998b). Drainages in separate grabens were not connected to form the Rio Grande River until ~2 Ma (Muehlberger and Dickerson 1989). Hot springs, including the Hot Springs in Big Bend National Park, issue from normal faults in Rio Grande River area grabens (Chesser and Estep 1986).

The south side of the Terlingua uplift contains five narrow, 0.5 km-wide, northwest-striking grabens (Erdlac 1990). The two richest cinnabar mines of the Terlingua mining district are located where grabens intersect the Laramide Terlingua monocline (Sharpe 1980). Cinnabar precipitated from hydrothermal fluids probably generated by nearby mid-Tertiary igneous intrusions (Sharpe 1980; Henry 1996).

Three major west-trending subvertical fault zones show evidence of right-lateral strike-slip and oblique-slip movement, postdating previously described Laramide and older displacement. Right-lateral offset is best documented on the Tascotal Mesa fault (Fig. 2) which offsets a Tertiary volcanic unit laterally one kilometer and contains subhorizontal slickenlines on fault surfaces (Henry 1998a). Erickson (1953) documented 200 meters of vertical displacement

on the fault, which suggests the fault has a multiphase movement history. The Redford-Lajitas fault zone is an east-striking zone of west-northwest-trending faults adjacent to and lining up with the Terlingua monocline (Fig. 2; Henry 1998a). The en echelon arrangement of faults within and slickenline rakes of mostly less than 45° document a component of right-lateral strike-slip offset. Vertical displacements on individual faults range up to 300 meters. The Chalk Draw fault (Fig. 2) has been interpreted to accommodate minor right-lateral and normal offset during Basin and Range deformation (Henry 1998a), although offset landforms suggest two kilometers of right-lateral offset (Dickerson and Muehlberger 1994). The northwest-trending west end of the fault shows normal fault offset of ~550 km (Cobb and Poth 1980; Scott, et al. 2004).

Northwest-trending right-lateral strike-slip faults have been described in Sierra del Carmen and in the Redford-Lajitas fault zone. In the Boquillas Canyon area (Fig. 2) northwest-striking right-lateral strike-slip faults bound the Dead Horse graben accommodation zone which links two north-northwest-striking normal faults that dip in opposing directions (Maler 1990). Figure 4 shows a well-exposed fault surface containing white calcite mineralization displaying extensive subhorizontal slickenlines indicating strike-slip offset (Maler 1990; Muehlberger and Merritt 1985). The six N75W-trending zones of northwest-trending en echelon faults in Sierra del Carmen are interpreted to accommodate a component of right lateral slip (Moustafa 1988). The Redford-Lajitas fault zone is a west-trending fault zone of en echelon oblique-slip faults containing fault surfaces indicating strike-slip and normal offset (Henry 1998a, 1998b).

Northeast-striking normal faults bound narrow grabens in the Delaware basin, northeast of Van Horn, Texas (north of Big Bend region). Faults strike N60E on average, dip 50 – 65°, and show 15 – 17 m displacement. These faults control the locations of several large commercial sulfur deposits (Hentz and Henry 1989). In this area, northeast-striking normal faults terminate at north-northwest-striking normal faults, indicating northeast-trending faults formed later. Near Van Horn correlative northeast- and east-northeast-trending, steeply dipping veins contain silver-copper-lead ore precipitated from hydrothermal fluids that moved upward along fractures (Price, et al. 1985). In the eastern Dog Canyon-Dagger Mountain area, possibly correlative northeast-trending fractures contain uneconomic amounts of cinnabar (Sharpe 1980; Daugherty 1981).

Folds. Folds generated during regional extension or caused by tension are harder to explain and less well known than folds formed during regional contraction. Nonetheless, folds of several styles and orientations deform post-Laramide Tertiary rocks and are near Basin and Range faults. Drag folds¹⁸ caused by Basin and Range normal and strike-slip fault movement are the first widespread fold type (Cooper, et al. 2008; Steven and Stevens 1989a). Normal offset on the eastern Chalk Draw fault (Fig. 2) displaced the Oligocene Rosillos laccolith and warped Cretaceous Pen formation beds from near horizontal to >75° within 0.5 km of the fault (Scott, et al. 2004). Right-lateral offset on the Tascotal Mesa fault (Fig. 2) deflected Tertiary volcanoclastic rocks 120° clockwise within 50 m of the fault (Henry 1998a). Drag fold monoclines in the hanging wall of the Sierra del Carmen fault east of Boquillas (Fig. 2) trend northwest, unlike adjacent Laramide folds (Carpenter 1997). Similarly, in the Dog Canyon-

¹⁸ Drag folds are warps adjacent to a fault produced by fault movement. Beds in the downthrown side adjacent to a normal fault are dragged upward while beds in the upthrown side are dragged downward.

Dagger Mountain area (Fig. 2), northwest-trending map-scale and outcrop-scale folds in Cretaceous rocks typically adjacent to Basin and Range normal faults are interpreted to be Basin and Range folds. Orientations of these folds differ from north-northwest-trending Laramide folds in this area (Satterfield and Dyess 2007).

Broad map-scale synclines that occupy long axes of narrow grabens (Fig. 5) are a second style of Basin and Range folds. These synclines apparently formed by drag on graben-bounding faults, resulting in sags in graben centers. The northwest-trending, 1.5 km-long Canoe syncline is particularly well exposed in three dimensions (Figs. 2, 5). This fold is defined by warps of the 51 – 47 Ma, post-Laramide Canoe Formation (Lehman 1991, 2004; Maxwell, et al. 1967, Stevens and Stevens 1989a). The north-northwest-trending, 8 km-long Black Gap syncline (Fig. 2) folds 22 Ma basaltic lava flows within the Black Gap graben (St. John 1966; Surpless 2007). The north-northwest-trending, 5 km-long Colquitt syncline, 25 km north of the Presidio bolson, folds Cretaceous, sedimentary rocks and Eocene and Oligocene (56 – 23 Ma) volcanic rocks (Twiss 1959; Henry and Price 1986). Rare “rollover” anticlines¹⁹ in downthrown blocks of normal faults are a third style of Basin and Range folds. A rollover anticline is adjacent to a bounding fault of the Castelon graben (Henry 1998a). A northwest-trending 30 kilometer-long gentle anticline north of the western Chalk Draw fault that folds 27 – 28 Ma volcanic rocks (Fig. 2; Goldich and Seward 1948; Erickson 1953; Stevens and Stevens 1985) may also be a rollover anticline. Relatively tight folds that may have formed by local compression at fault bends are a fourth style of Basin and Range folds. A tight east-northeast-trending anticline and syncline adjacent and oblique to the Tascotal Mesa fault deform Tertiary volcanoclastic rocks (Henry 1998a). Broad west-trending synclines in a graben within the Redford -Lajitas fault zone in Tertiary volcanic rocks (Henry 1998a) may have formed in this way. Fault propagation folds, a fifth Basin and Range fold type, are represented in Sierra del Carmen by a large monocline draped over a well-exposed normal fault with 300 m offset (Ferrill, et al. 2004). In a similar way, map-scale Chihuahua thrust belt folds, including the Sierra Grande fold (Fig. 1), are reoriented from northwest-trending to north-northwest-trending west of the western termination of the Tascotal Mesa fault (Muehlberger 1989; Henry 1998a).

Phases and timing of deformation. First-phase east-northeast extension, which produced nearly all Basin and Range faults and folds in the Big Bend region, began as early as 31 Ma. Dikes whose orientation indicates regional Basin and Range extension are well documented to be 28 Ma old; some may be as old as 31 Ma (Henry and Price 1986; Price and Henry 1985). Dated veins formed during east-northeast extension in five mining districts northern Mexico are 27 – 32 Ma (Henry and Aranda-Gomez 1992) In the Castelon graben, a 28 Ma pluton intruded along a Basin and Range normal fault, establishing that this fault moved prior to 28 Ma (Stevens and Stevens 1990b; Dickerson and Muehlberger 1994). Lava flows in basal graben fill deposits have been dated at 23 Ma, meaning extension must have been underway by then (Price and Henry 1995). The oldest rift basin sediments dated by vertebrate fossils are about the same age (Stevens and Stevens 1985, 1989b; Dickerson and Muehlberger 1994). The Black Gap syncline and synchronous basin-bounding faults were active at the same

¹⁹ Rollover anticlines are anticlines in the downthrown upper plate of a normal fault produced by fault movement. They are also called “reverse drag folds” because the fold limb adjacent to the fault dips towards the fault, unlike typical drag folds.

approximate time: 22 Ma basalt flows are folded and increase in number and thickness in the center of the syncline (Surpless 2007; St. John 1966).

A second phase of northwest extension began about 10 Ma and continues today along several zones of active faults. Graben-bounding faulting has been documented at 10 – 9 Ma, the age of oldest deposits in the Tornillo graben, and at less than 2 Ma (Stevens and Stevens 1985, 1989b). Most known active faults²⁰, lines containing hatchures on Figure 2, are along the western margin of the Big Bend near the Rio Grande River (Muehlberger, et al. 1978; Henry, et al. 1985). Several active faults have been identified along the eastern margin in and near Sierra del Carmen (Fig. 2; Collins 1994; Stevens 1994). Faults have been identified by applying several criteria. First, active or potentially active faults offset Quaternary sediments (large areas of Quaternary and Tertiary sediments are shown in yellow on Figure 2). Active graben-bounding faults in the Presidio and Redford bolsons, including the Tascotal Mesa fault, juxtapose Quaternary sediments against Tertiary igneous and Cretaceous sedimentary rocks (Dickerson 1996; Dickerson and Muehlberger 1994). The Dugout Wells fault (Fig. 2) near southern Sierra del Carmen offsets Quaternary caliche deposits (Stevens 1994). Several faults near Boquillas Canyon area offset Late Cenozoic, possibly Quaternary-age gravels (Maler 1990). Second, steep, planar, little-eroded fault scarps (criterion described by Wallace, 1978) are characteristic of Big Bend region active faults (Muehlberger, et al. 1978). Third, earthquake epicenters from 1976 to 1980 plot in a diffuse belt along the Rio Grande, mostly north of the Presidio bolson; several quakes were recorded in the Black Gap area in the eastern Sierra del Carmen (Dumas, 1980). The Magnitude ~6.4 1931 Valentine earthquake, the largest in Texas in historical time, displayed right-lateral strike-slip motion, possibly on the northwest-striking Valentine fault (north of Figure 2; Doser 1987; Muehlberger and Dickerson 1989).

In the Dog Canyon-Dagger Mountain area, northwest-striking high-angle faults crosscut the South Persimmon Gap laccolith. Assuming that the laccolith is the same age as nearby dated plutons (31 – 32 Ma; Morgan, et al. 2006; Miggins, et al. 2006), then these faults must have moved after 32 Ma. Probable fault movement in the Quaternary Period in this area is documented by northwest- and north-northwest-striking normal and right-oblique-slip faults that display linear scarps and juxtapose Quaternary alluvium and talus against Cretaceous limestone.

Orientations of dikes, veins, faults, and slickenlines on fault surfaces indicate two phases of extension. Dikes intruded from 31 to 17 Ma (the youngest igneous rocks known) throughout the Big Bend region are dominantly oriented north-northwest, indicating regional east-northeast extension was responsible for opening fractures now filled with intrusive igneous rock (Price and Henry 1985; Henry, et al. 1991). Numerous slickenline and fault surface orientations analyzed using the paleostress technique of Angelier (1979) also yield fairly consistent east-northeast and northeast extension directions. Slickenline data include six locations around the Tascotal Mesa and Redford-Lajitas fault zones (Henry, 1998a, 1998b), Sierra Azul, south of the Redford graben (Henry, et al. 1991), and in the Van Horn area (Price, et al. 1985). Consistent orientations over a large area suggest that east-northeast extension was the dominant phase. A second phase of northwest extension is documented by sparse northeast-striking normal faults that postdate north-northwest-striking faults in the Delaware basin (Hentz and Henry 1989), by northeast-striking veins in the Van Horn area, and by fault surface and slickenline data in the Van Horn area (Price,

²⁰ Active and potentially active faults have moved at some time in the Quaternary Period, from 1.8 Ma until present.

et al. 1985). Strike-slip offset on northwest- and north-northwest-striking faults is also consistent with second-phase northwest extension on earlier-formed faults.

Interpretations. Data on Basin and Range structures have led to three straightforward interpretations. First, many Basin and Range faults are interpreted to be reactivated Laramide and older faults. In the Santiago Mountains, a Basin and Range normal fault and a nearby parallel Laramide thrust fault are interpreted to share the same fault plane at depth. In this model only the steep portion of a steepening downward thrust is reactivated as a normal fault (Cobb and Poth 1980). Major west-striking fault zones, active in the Paleozoic, were reactivated during Laramide and Basin and Range mountain-building. The right-oblique Redford-Lajitas fault zone (Fig. 2), a Basin and Range structure (Henry 1998a), lines up with and is interpreted to have reactivated the basement fault that created the Laramide Terlingua monocline (Fig. 1). Moustafa (1988) interpreted that west-northwest-trending en echelon fault zones in Sierra del Carmen first accommodated a component of left-lateral displacement during the Laramide orogeny followed by right-lateral displacement during Basin and Range extension. The Muskog Spring normal fault in Sierra del Carmen is interpreted to be a reactivated Laramide fault because outcrop-scale Laramide folds are concentrated near the fault (Satterfield, et al. 2008).

Second, the overall amount of extension in the Big Bend region is interpreted to be small, 5 – 30% (Henry 1998a; Henry and Price 1986), which is about the same extension amount as for fault block mountains elsewhere in the Basin and Range outside small areas of extreme extension. Because large graben-bounding faults are steep, they have accommodated large vertical displacements and produced high escarpments without extending the area greatly. This interpretation is supported by the consistent orientation of Laramide folds over large parts of Sierra del Carmen, which indicates that these structures have not been rotated or tilted greatly during Basin and Range extension (Satterfield, et al. 2008). The rarity of steep dips in post-Laramide strata and the scarcity of rollover anticlines in upper plates of normal faults suggest that faults do not curve and become subhorizontal with depth. The small Dead Horse graben in Boquillas Canyon (Fig. 2) is a local exception where bounding faults are interpreted to become subhorizontal at the base of the Cretaceous section (Maler 1990).

Third, Basin and Range normal faults, strike-slip faults, and folds have been interpreted to comprise one or several right-lateral transtensional fault zones in which faults are linked in networks that move synchronously (e.g. Tauvers and Muehlberger 1989; Cobb and Poth 1980). The cause of transtension in this region is straightforward: most existing faults are not orthogonal to extension directions, meaning that when existing faults move there can be a strike-slip component and a normal component of displacement. How components are distributed remains to be determined; does each fault move as an oblique-slip fault, or are displacements partitioned such that some faults are primarily strike-slip faults and others normal faults? Also, the relative significance and timing of the strike-slip component on northwest-trending faults is poorly understood: is it a component of early-phase east-northeast extension, and/or is it caused by late-phase, post 10 Ma northwest extension?

Causes of extension and transtension

At least four hypotheses explaining extension in the Basin Range province have been proposed (detailed descriptions in Wernicke (1992)). One model proposes that over-thickening the lithosphere by contraction during Cordilleran mountain-building eventually triggered spreading under its own weight, including extension in the crust (Coney and Harms 1984). The timing and locations of first-phase, extreme extension, mostly after contraction ended and in the same areas, support this model. In addition, variable early extension directions are generally perpendicular to the boundaries of shortened areas (Wernicke 1992). An alternative hypothesis proposes that post-Laramide steepening of the shallow subducted Farallon plate could allow hot asthenosphere to rise under the crust, triggering igneous activity. Resulting hot asthenosphere and lower lithosphere would weaken the crust, triggering extension (e.g. Burchfiel, et al. 1992). Convection currents in the asthenosphere could provide forces causing extension (Wernicke 1992). This model explains the return of igneous activity throughout the Laramide orogen after a lull from 70 Ma to 40 Ma. Second- and third-phase extension and transtension is related to the change in plate boundary type from convergent to transform and the birth of the San Andreas transform fault zone (Burchfiel, et al. 1992; Dickinson 2006; Price and Henry 1985; Zoback, et al. 1981). The shift in extension direction from east-northeast to northwest at about 10 Ma appears related to the lengthening of the San Andreas fault to the south and the change from convergent to transform plate boundary setting of Baja California area at that time (Wernicke 1992; Henry and Aranda-Gomez 1992).

KEY POINTS

Figures 1 and 2 display a complex array of Laramide and Basin and Range structures of diverse styles, phases, and orientations. This paper summarizes what is known about these structures and how they have been interpreted. When Big Bend Laramide and Basin and Range structures are compared with structures of the same age elsewhere in North America several points stand out:

1) Laramide basement uplifts are not confined to the Wyoming-Colorado-New Mexico area. As in better known areas of the Laramide orogen, the Big Bend region contains a characteristic Laramide basement uplift, the Marathon-El Burro-Peyotes uplift, a flanking basin, the Tornillo basin, and other structures produced by one main phase of northeast-southwest shortening from ~70 – 50 Ma. The Dog Canyon overturned syncline (Fig. 3) is a particularly well exposed example of a fold on the flank of the Marathon-El Burro-Peyotes uplift. As in better known areas of the Laramide orogen, the structures in the Laramide-style, thick-skinned Marathon-El Burro-Peyotes uplift were active at the same time as the thin-skinned Chihuahua tectonic belt to the west.

2) As in the Great Basin, the best studied part of the Basin and Range Province, the Big Bend region contains fault block mountains and intervening basins bounded by range front normal faults that accommodated 5 – 30% extension. Unlike in the Great Basin, local areas of extreme extension have not been identified in the Big Bend region. The Walker Lane belt and the Texas Lineament are similar ~200 km-wide belts of transtensional structures within the Basin and

Range Province. The Walker Lane has accommodated ~65 km of right-lateral displacement, while strike-slip displacement amounts on the Texas Lineament overall are poorly constrained and perhaps less. The Big Bend region contains two broad belts of active faults, although in historical time earthquakes are smaller and less frequent than in the Great Basin and Walker Lane.

3) The dominant phase of extension on high-angle normal faults in the Big Bend region was east-northeast extension from ~30 – 10 Ma, while northwest extension after 10 Ma produced Great Basin fault block mountains. Active faults in the Big Bend region cluster along the course of the Rio Grande River.

4) Map-scale and outcrop-scale folds that formed during Basin and Range extension are widespread throughout the Big Bend region. The Canoe syncline (Fig. 5) is a particularly well-exposed and accessible example.

5) As in the better known areas of the Laramide orogen and Basin and Range province, Big Bend region Laramide and Basin and Range structures include strike-slip faults and a strike-slip component on reverse or normal faults. The exceptionally well-exposed fault in Boquillas Canyon (Fig. 4) is a good example. Left-lateral strike-slip faults may link together with Laramide thrust faults to form transpressional flower structures. Right-lateral strike-slip faults may link together with Basin and Range normal faults to form transtensional flower structures.

6) As in the Walker Lane belt in the western Great Basin, many significant Big Bend region and Basin and Range faults are reactivated Mesozoic and Paleozoic structures. Paleostress directions not at right angles to existing faults produced strike-slip components of displacements. The west-striking Chalk Draw and Tascotal Mesa faults (Figs. 1, 2) which were subparallel to east-northeast Laramide compression and east-northeast Basin and Range extension are particularly well-documented reactivated structures.

7) Locations of mountain ranges, ore deposits, springs, and the Rio Grande River in the Big Bend region are controlled by Laramide and Basin and Range folds and faults.

APPENDIX: PANORAMIC PHOTOGRAPHY

Landscape photography for documentary purposes has been conducted since the advent of photographic process in 1839. Photography now can be easily employed by any field-based scientist wishing to use this tool to record their research (Ashmore 2006). Panoramic photography allows for an expanded view beyond what one could normally see from one vantage point. The simplest way to produce a panoramic photograph is to stand and take a series of photographs from one location by recording images that slightly overlap each other. Once printed, the photos can be pieced together to produce the expanded horizontal and/or vertical image. Of course overlap problems, called parallax errors, will be evident, especially with objects in images that are less than 300 m from the camera. Use of a tripod can help to eliminate some parallax errors.

The recent advent of digital cameras and specialty computer programs allow for the production of very inexpensive panoramic photographs with little or no visible parallax errors. Depending on the resolution of the camera's sensor and printing capabilities available to the photographer, panoramic photographs can be produced that measure in excess to 8 m long and 4.5 m high. To produce such images, it is strongly suggested to use a tripod that allows for the camera to be panned left-to-right and up-and-down (if vertical and/or multi-row photographs are desired). Each image photographed should be overlapped 30-50%, to allow the computer program a generous opportunity to acquire common points within each set of adjacent photographs for aid in stitching the images together. There are a host of quality, stand-alone programs available online that will morph images together to produce an image that is practically seamless. Such programs include PanaVue ImageAssembler (<http://www.panavue.com>) and PTGui (<http://www.ptgui.com>). Photoshop CS3 and later versions (<http://www.adobe.com/products/photoshop/photoshopextended>) also have a quality image stitching tool as part of their program.

For panoramic images of landscapes further than 300 m from the camera, this procedure will work fine with little or no visible parallax errors. But, if one is wishing to produce very high resolution, fine detailed, large prints and/or images of subjects that are within 300 m of the camera without parallax errors, special positioning of the camera onto the tripod is necessary. In this case, the camera must be positioned onto the tripod such that as the camera is rotated right-to-left and tilted up-and-down the point where light strikes the sensor or film is not moving. This point is called the nodal point. With a tripod head specially designed for photographing panoramic photographs, centering the nodal point over the axis of rotation of the camera for a particular camera lens is not difficult. Hamblenne (2004) provides an excellent discussion of how to find and center a camera's nodal point for any size lens. One drawback to this process is the monetary costs of the tripod and specialty panoramic tripod head. Since professional equipment is required, the cost of such a tripod set-up (not considering the camera) can easily range between \$700.00 and \$2,000.00. The company Really Right Stuff (<http://reallyrightstuff.com/home.html>), produces high-end, rugged tripod heads that allow for precise horizontal and vertical positioning of the camera onto the tripod. Although not inexpensive, the ease of set-up and quality of images produced with this type of equipment are very impressive.

REFERENCES

- Anderson, T.H., and V.A. Schmidt. 1983. The evolution of Middle America and the Gulf of Mexico-Caribbean Sea region during Mesozoic time. *Geological Society of America Bulletin* 94: 941 – 966.
- Angelier, J. 1979. Determination of the mean principal directions of stresses for a given fault population. *Tectonophysics* 56: T17 – T26.
- Armstrong, R.L. 1982. Cordilleran metamorphic core complexes – From Arizona to southern Canada. *Annual Reviews of Earth and Planetary Science* 10: 129 – 154.
- Ashmore, R.A. 2006. Production and Use of Large-Scale Panoramic Photography in Field Based Sciences. *Programs and Abstracts of the 109th Annual Meeting of the Texas Academy of Science*: 75. http://www.texasacademyofscience.org/2006_tas_program.pdf. (accessed September 2008).
- Bates, R.L., and J.A. Jackson, eds. 1984. *Dictionary of geological terms, third edition*. New York, New York: Doubleday.
- Berge, T.B. 1984. Structural evolution of the Chihuahua tectonic belt, Trans-Pecos Texas. *West Texas Geological Society Bulletin* 23: 7 – 13.
- Bird, P. 1998. Kinematic history of the Laramide orogeny in latitudes 35°-49°N, western United States. *Tectonics* 17: 780 – 801.
- Brister, B.S. 1986. *Structural geology of the Horse Peak area, southern Eagle Mountains* [Master's thesis]. Alpine, Texas: Sul Ross State University.
- Bumgardner, J.E. 1976. *Geology of the gabbro sill surrounding Mariscal Mountain, Big Bend National Park, Texas* [Master's thesis]. Austin: University of Texas at Austin.
- Burchfiel, B.C., D.S. Cowan, and G.A. Davis. 1992. Tectonic overview of the Cordilleran orogen in the western United States, in Burchfiel, B.C., P.W. Lipman, and M.L. Zoback, eds. *The Cordilleran orogen: Conterminous U.S. Boulder Colorado*, Geological Society of America, The Geology of North America G-3: 407 – 479.
- Carpenter, D.L. 1997. Tectonic history of the metamorphic basement rocks of the Sierra del Carmen, Coahuila, Mexico. *Geological Society of America Bulletin* 109: 1321 – 1332.
- Caskey, S.J., S.G. Wesnousky, P. Zhang, and D.B. Slemmons. 1996. Surface faulting of the 1954 Fairview Peak (M_s 7.2) and Dixie Valley (M_s 6.8) earthquakes, central Nevada. *Bulletin of the Seismological Society of America* 86: 761 – 787.

- Chapin C.E. and S.M. Cather. 1983. Eocene tectonics and sedimentation in the Colorado Plateau – Rocky Mountain area, in Lowell, J.D., and R. Gries, eds. *Rocky Mountain foreland basins and uplifts*. Denver Colorado, Rocky Mountain Association of Geologists: 33 - 56.
- Charleston, S. 1981. A summary of the structural geology and tectonics of the state of Coahuila, Mexico in Schmidt, C.I. and Katz, S.B., eds. *Lower Cretaceous stratigraphy and structure, northern Mexico*. Midland, Texas: West Texas Geological Society Field Trip Guidebook, Publication 81-74: p. 28 – 36.
- Chávez, G. 2008. The Laramide orogeny in Mexico: An updated revision. *Geological Society of America Abstracts with Programs* 40.
- Chávez, G., J. Aranda, A. Iriondo, M. Aranda, R. Peterson, and S. Eguiluz. 2008. Evidence of basement inversion during the Laramide orogeny in the Sabinas basin area, Coahuila, Mexico. *Geological Society of America Abstracts with Programs* 40.
- Chávez-Cabello, G., J.J. Aranda-Gómez, R.S. Molina-Garza, T. Cossío-Torres, I.R. Arvizu-Gutiérrez, and G.A. González-Naranjo. 2007. The San Marcos fault: A Jurassic multireactivated basement structure in northeastern México, in Alaniz-Alvarez, S.Á. and Nieto-Samaniego, Á.F., eds. *Geology of México: Celebrating the Centenary of the Geological Society of México*. Boulder, Colorado: Geological Society of America Special Paper 442. p. 261 – 286.
- Chesser, K. and J.D. Estep. 1986. Hot Springs of Big Bend National Park and Trans-Pecos Texas, in Pause, P.H., and R.G. Spears, eds. *Geology of the Big Bend area and Solitario dome, Texas*. Midland, Texas, West Texas Geological Society 1986 Field Trip Guidebook, Publication 86-82: 96 – 104.
- Clement, J.H. 1983. North flank of the Uinta Mountains, Utah, in Bally, A.W., ed. *Seismic expression of Structural Styles, A picture and work atlas, Volume 3*. Tulsa, Oklahoma, American Association of Petroleum Geologists Studies in Geology #16: 29 – 32.
- Cobb, R.C. and S. Poth. 1980. Superposed deformation in the Santiago and northern Del Carmen Mountains, Trans-Pecos Texas, in Dickerson, P.W., and J.M. Hoffer, eds. *Trans-Pecos region, southeastern New Mexico and West Texas*. Socorro, New Mexico: New Mexico Geological Society, 31st Field Conference Guidebook: 71 – 75.
- Collins, E.E., compiler. 1995. Fault number 917, Unnamed fault east of Santiago Peak, in Quaternary fault and fold database of the United States. <http://earthquakes.usgs.gov/regional/qfaults> (accessed November 13, 2006).
- Cooper, R.W., D.A. Cooper, J.B. Stevens, and M.S. Stevens. 2008. Structural geology of the Late Cretaceous Boquillas Formation, eastern Big Bend National Park (Solis to Persimmon Gap), Trans-Pecos, Texas. *Geological Society of America Abstracts with Programs* 40.

- Coney, P.J. and T.A. Harms. 1984. Cordilleran metamorphic core complexes: Cenozoic extensional relics of Mesozoic compression. *Geology* 12: 550 – 554.
- Corry, C.E., E. Herrin, F.W. McDowell, K.A. Phillips. 1990. *Geology of the Solitario, Trans-Pecos Texas*. Boulder, Colorado, Geological Society of America Special Paper 250. geologic map scale 1:24,000.
- Corry, C.E., J.B. Stevens, and E. Herrin. 1994. A Laramide age push-up block: The structures and formation of the Terlingua-Solitario structural block, Big Bend region, Texas: Discussion. *Geological Society of America Bulletin* 106: 553 – 556.
- Daugherty, F.W. 1963. La Cueva intrusive complex and dome, northern Coahuila, Mexico. *Geological Society of America Bulletin* 74: 1429 – 1438.
- Daugherty, F.W. 1981. Mineral resources of Brewster – Presidio Counties, Texas, in Jons, R.D., P.H. Muller, and W.R. Gibson, eds. *Marathon – Marfa region of West Texas Symposium and Guidebook*. Midland Texas: Permian Basin Section Society of Economic Paleontologists and Mineralogists Publication 81-20: 210 – 214.
- Davis, G.H. and S.J. Reynolds. 1996. *Structural Geology of Rocks and Regions, 2nd Edition*. Hoboken, New Jersey: John Wiley & Sons, Inc.
- DeFord, R.K. and W.T. Haenggi. 1970. Stratigraphic nomenclature of Cretaceous rocks in northeastern Chihuahua, in Seewald, K., and D. Sundeen, eds. *The geologic framework of the Chihuahua tectonic belt*. Midland, Texas: West Texas Geological Society: 175 – 196.
- Denison, R.E., W.H. Burke, Jr., E.A. Hetherington, and J.B. Otto. 1970, Basement rock framework of parts of Texas, southern New Mexico and northern Mexico, in Seewald, K., and D. Sundeen, eds. *The geologic framework of the Chihuahua tectonic belt*. Midland, Texas: West Texas Geological Society: 3 - 14.
- DeCamp, D.W. 1985. Structural geology of Mesa de Anguila, Big Bend National Park, in Dickerson, P.W. and W.R. Muehlberger, eds., *Structure and tectonics of Trans-Pecos Texas*. Midland, Texas: West Texas Geological Society Field Conference, Publication 85-81: 127 – 135.
- Dickerson, P.W. 1980. Structural zones transecting the southern Rio Grande rift – Preliminary observations, in Dickerson, P.W. and J.M. Hoffer, eds. *Trans-Pecos region, southeastern New Mexico and West Texas*. Socorro, New Mexico: New Mexico Geological Society 31st Field Conference Guidebook: 63 - 70.
- Dickerson, P.W. 1981. Evidence for basement control of structural zones transected by the southern Rio Grande rift, in Gabrielson, R.H., I.B. Ramberg, D. Roberts, and O.A. Steinlein, eds. *Proceedings of the fourth international conference on basement tectonics*. Salt Lake City, Utah: International Basement Tectonics Association Publication No. 4: 103 – 114.

- Dickerson, P.W. 1985. Evidence for late Cretaceous – early Tertiary transpression in Trans-Pecos Texas and adjacent Mexico, *in* Dickerson, P.W. and W.R. Muehlberger, eds. *Structure and tectonics of Trans-Pecos Texas*. Midland, Texas: West Texas Geological Society Field Conference, Publication 85-81: 185 - 194.
- Dickerson, P.W. 1996. Late Paleozoic through Quaternary activity on Tascotal Mesa fault zone, Big Bend region of West Texas and Chihuahua. *Geological Society of America Abstracts with Programs* 28: A-448.
- Dickerson, P.W. and W.R. Muehlberger. 1994. Basins in the Big Bend segment of the Rio Grande rift, Trans-Pecos Texas, *in* Keller, G.R. and S.M. Cather, eds. *Basins of the Rio Grande Rift: Structure, stratigraphy, and tectonic setting*. Boulder, Colorado: Geological Society of America Special Paper 291: 283 - 297.
- Dickinson, W.R. 2006. Geotectonic evolution of the Great Basin. *Geosphere* 2: 353 – 368.
- Dickinson, W.R. and W.S. Snyder. 1978. Plate tectonics of the Laramide orogeny, *in* Matthews, V., III, ed. *Laramide folding associated with basement block faulting in the western United States*. Boulder, Colorado: Geological Society of America Memoir 151: 355 – 366.
- Dickinson, W.R., and six others. 1988. Paleogeographic and paleotectonic setting of Laramide sedimentary basins in the central Rocky Mountain region. *Geological Society of America Bulletin* 100: 1023 – 1039.
- Dohrenwend, J.C. 2002. Satellite imaging of national parklands in the arid Southwest. *Geological Society of America Abstracts with Programs* 34.
- Doser, D.I. 1987. The 16 August 1931 Valentine, Texas Earthquake: Evidence for normal faulting in West Texas. *Bulletin of the Seismological Society of America* 77: 2005 – 2017.
- Dumas, D.B. 1980. Seismicity in the Basin and Range Province of Texas and northeastern Chihuahua, Mexico, *in* Dickerson, P.W. and J.M. Hoffer. eds. *Trans-Pecos region, southeastern New Mexico and West Texas*. Socorro, New Mexico: New Mexico Geological Society, 31st Field Conference Guidebook: 77 – 81.
- Edwards, K. and R.M. Batson. 1990. *Experimental digital shaded-relief maps of Nevada*. Denver, Colorado: U.S. Geological Survey Miscellaneous Investigations Series Map I – 1849: scale 1:1,000,000.
- English, J. and S. Johnston. 2004. The Laramide Orogeny: What were the Driving Forces? *International Geology Review* 46: 833-838.
- Erdlac, R.J., Jr. 1990. A Laramide-age push-up block: The structures and formation of the Terlingua – Solitario structural block, Big Bend region, Texas. *Geological Society of America Bulletin* 102: 1065 – 1076.

- Erdlac, R.J., Jr. 1994. Laramide paleostress trajectories from stylolites in the Big Bend region, in Laroche, T.M. and J.J. Viveiros, eds. *Structure and tectonics of the Big Bend area and southern Permian basin, Texas*. Midland, Texas: West Texas Geological Society 1994 Field Trip Guidebook Publication 94 – 95: 165 – 187.
- Erdlac, R.J., Jr. 1996. Laramide deformation of the Solitario area, in Henry, C.D. and W.R. Muehlberger, eds. *Geology of the Solitario dome, Trans-Pecos Texas: Paleozoic, Mesozoic, and Cenozoic sedimentation, tectonism, and magmatism*: Austin Texas: Bureau of Economic Geology Report of Investigations No. 240: 47 - 57.
- Erdlac, R.J., Jr. 2002. The Terlingua monocline, in White, J.C., ed. *The geology of Big Bend National Park: What have we learned since Maxwell and others (1967)? Field Trip Guide*: Geological Society of America South-Central Meeting: p. 12 – 14.
- Erdlac, R.J., Jr. and C.D. Henry. 1994. A Laramide age push-up block: The structures and formation of the Terlingua-Solitario structural block, Big Bend region, Texas: Reply. *Geological Society of America Bulletin* 106: 557 – 559.
- Erickson, R.L. 1953. Stratigraphy and petrology of the Tascotal Mesa Quadrangle: *Geological Society of America Bulletin* 64: 1363 – 1386.
- Ewing, T.E. 1985. Westward extension of the Devils River uplift – Implications for the Paleozoic evolution of the southern margin of North America. *Geology* 13: 433 – 436.
- Ewing, T.E. 1991. The tectonic framework of Texas: Text to accompany “The Tectonic Map of Texas”. Austin, Texas: Bureau of Economic Geology, University of Texas at Austin.
- Ferrill, D.A., D.W. Sims, D.J. Waiting, A.P. Morris, N.M. Franklin, and A.L. Schultz. 2004. Structural framework of the Edwards Aquifer recharge zone in south-central Texas. *Geological Society of America Bulletin* 116: 407 – 418.
- Gilmer, A.K., J.R. Kyle, J.N. Connelly, R.D. Mathur, and C.D. Henry. 2003. Extension of Laramide magmatism in southwestern North America into Trans-Pecos Texas. *Geology* 31: 447 – 450.
- Goldich, S.S., and C.L. Seward. 1948. Green Valley – Paradise Valley trip, in Goldich, S.S., C.L. Seward, J.T. Lonsdale, R.K. DeFord, and G.K. Eifler, Jr., leaders. *Fall field trip, Green Valley and Paradise Valley, Wire Gap and the Solitario, Limpia Canyon and Barrilla Mountains*. Midland, Texas: West Texas Geological Society: 11 – 36.
- Gries, J.C. and W.T. Haenggi. 1970. Structural evolution of the Chihuahua tectonic belt, in Seewald, K. and D. Sundeen, eds. *The geologic framework of the Chihuahua tectonic belt*. Midland, Texas: West Texas Geological Society: 119 - 137.

- Gries, R. 1983. North-south compression of Rocky Mountain foreland structures, in Lowell, J.D. and R. Gries, eds. *Rocky Mountain foreland basins and uplifts*. Denver Colorado: Rocky Mountain Association of Geologists: 9 – 32.
- Grotzinger, J., T.H. Jordan, F. Press, and R. Siever. 2007. *Understanding Earth, Fifth Edition*. New York, New York: W.H. Freeman and Co.
- Hanson, R., K. Befus, J. Breyer, A. Busbey, T. Lehman, and D. Miggins. 2007. Newly recognized Cretaceous and Eocene basaltic phreatomagmatic volcanism in the Big Bend area, West Texas. *Geological Society of America Abstracts with Programs* 36: 511.
- Hardyman, R.F., and J.S. Oldow. 1991. Tertiary tectonic framework and Cenozoic history of the central Walker Lane, in Raines, G.L. and others, eds. *Geology and ore deposits of the Great Basin: Symposium proceedings*. Reno, Nevada: Geological Society of Nevada: 279 – 301.
- Harlan, S.S., J.W. Geissman, C.D. Henry, and T.C. Onstott. 1995. Paleomagnetism and $^{40}\text{Ar}/^{39}\text{Ar}$ geochronology of gabbro sills at Mariscal Mountain anticline, southern Big Bend National Park, Texas: Implications for the timing of Laramide tectonisms and vertical axis rotations in the southern Cordilleran orogenic belt. *Tectonics* 14: 307 – 321.
- Hamblenne, A. 2004. The Grid: Method for a Precise Location of the Entrance Pupil on a DSLR Camera. <http://www.outline.be/quiktime/tuto/TheGrid.pdf>. (accessed September 2008).
- Hazzard, R.T., R.A. Maxwell, J.T. Lonsdale, and trainees of the Gulf Oil Corporation. 1967. Geologic map of the Persimmon Gap – Dog Canyon area, Big Bend National Park, Brewster County, Texas, scale 1:9600, in Maxwell, R.A., J.T. Lonsdale, R.T. Hazzard, and J.A. Wilson. *Geology of Big Bend National Park, Brewster County, Texas*. Austin, Texas: Bureau of Economic Geology Publication 6711.
- Head, J.A. 2002. *Stratigraphic and structural controls of Permian carbonate-hosted silver (Pb-Zn) mineralization, Shafter, Presidio County, Texas* [Master's thesis]. Austin, Texas: University of Texas at Austin.
- Hennings, P.H., R. Dyer, and W.R. Muehlberger. 1989. Laramide development of the eastern Chihuahua tectonic belt, West Texas and Northeast Chihuahua, Mexico in Muehlberger, W.R. and P.W. Dickerson, eds. *Structure and Stratigraphy of Trans-Pecos Texas: Field Trip Guidebook T317, 28th International Geological Congress*. Washington D.C.: American Geophysical Union, 71 – 85.
- Hennings, P.H. 1994. Structural transect of the southern Chihuahua Fold Belt between Ojinaga and Aldama, Chihuahua, Mexico. *Tectonics* 13: 1445 – 1460.

- Henry, C.D. 1996. Economic Geology, in Henry, C.D. and W.R. Muehlberger, eds., *Geology of the Solitario dome, Trans-Pecos Texas: Paleozoic, Mesozoic, and Cenozoic sedimentation, tectonism, and magmatism*: Austin, Texas: Bureau of Economic Geology Report of Investigations No. 240: 146 -150.
- Henry, C.D. 1998a. Basement-controlled transfer zones in an area of low-magnitude extension, eastern Basin and Range province, Trans-Pecos Texas, in Faults, J.E. and J.H. Stewart, eds. *Accommodation zones and transfer zones: The regional segmentation of the Basin and Range province*. Boulder, Colorado: Geological Society of America Special Paper 323: 75 – 88.
- Henry, C.D. 1998b. *Geology of Big Bend Ranch State Park, Texas*. Austin, Texas: Bureau of Economic Geology Guidebook 27. map scale 1:50,000.
- Henry, C.D. and J.J. Aranda-Gomez, J.J. 1992. The real southern Basin and Range; mid- to late Cenozoic extension in Mexico. *Geology* 20: 701 – 704.
- Henry, C.D. and F.W. McDowell. 1986. Geochronology of magmatism in the Tertiary volcanic field , Trans-Pecos Texas in Price, J.G., C.D. Henry, D.F. Parker, and D.S. Barker, eds. *Igneous geology of Trans-Pecos Texas: Field trip guide and research articles*. Austin, Texas: Bureau of Economic Geology Guidebook 23: 99 – 122.
- Henry, C.D., and R.J. Erdlac Jr. 1996. Basin and Range fault system, in Henry, C.D. and W.R. Muehlberger, eds., *Geology of the Solitario dome, Trans-Pecos Texas: Paleozoic, Mesozoic, and Cenozoic sedimentation, tectonism, and magmatism*. Austin, Texas: Bureau of Economic Geology Report of Investigations No. 240: 137 - 143.
- Henry, C.D., and R.J. Erdlac Jr. 1996. Black Mesa dome and intrusion, in Henry, C.D. and W.R. Muehlberger, eds., *Geology of the Solitario dome, Trans-Pecos Texas: Paleozoic, Mesozoic, and Cenozoic sedimentation, tectonism, and magmatism*. Austin, Texas: Bureau of Economic Geology Report of Investigations No. 240: 105 – 108.
- Henry, C.D., and W.R. Muehlberger. 1996. Structure of the Solitario dome and caldera in Henry, C.D. and W.R. Muehlberger, eds., *Geology of the Solitario dome, Trans-Pecos Texas: Paleozoic, Mesozoic, and Cenozoic sedimentation, tectonism, and magmatism*. Austin, Texas: Bureau of Economic Geology Report of Investigations No. 240: 121 – 136.
- Henry, C.D. and J.G. Price. 1985. *Summary of the tectonic development of Trans-Pecos Texas*. Austin, Texas: Bureau of Economic Geology Miscellaneous Map No. 36: map scale 1:100,000.
- Henry, C.D. and J.G. Price. 1986. Early Basin and Range development in Trans-Pecos Texas and adjacent Chihuahua: Magmatism and orientation, timing, and style of extension. *Journal of Geophysical Research* 91: 6213 – 6224.

- Henry, C.D. and J.G. Price. 1989. The Christmas Mountains caldera complex, Trans-Pecos Texas: Geology and development of a laccocaldera. *Bulletin of Volcanology* 52: 97 – 112.
- Henry, C.D., J.G. Price, and D.E. Miser. 1989. *Geology and Tertiary igneous activity of the Hen Egg Mountain and Christmas Mountains Quadrangles, Big Bend region, Trans-Pecos Texas*. Austin, Texas: Bureau of Economic Geology Report of Investigations No. 183: 105 p., map scale 1: 24,000.
- Henry, C.D., J.G. Price, and E.W. James. 1991. Mid-Cenozoic stress evolution and magmatism in the southern Cordillera, Texas and Mexico: Transition from continental arc to intraplate extension. *Journal of Geophysical Research* 96: 13545-13560.
- Hentz, T.F. and Henry, C.D., 1989, Evaporite-hosted native sulfur in Trans-Pecos Texas: Relation to late-phase Basin and Range deformation. *Geology* 17: 400 – 403.
- Jacquot, J. 1978. *Geology of the Eastern Half of the Bullis Gap Quadrangle, West Texas* [M.A. Thesis]. Austin, Texas: University of Texas at Austin.
- Kesler, S.E. 1977. Geochemistry of manto fluorite deposits, northern Coahuila, Mexico. *Economic Geology* 72: 204 – 218.
- King, P. B. 1937. *Geology of the Marathon region, Texas*. Denver, Colorado: U.S. Geological Survey Professional Paper 187. map scale 1: 125,000.
- King, P.B. 1980. *Geology of the eastern part of the Marathon basin, Texas*. Denver, Colorado: U.S. Geological Survey Professional Paper 1157. map scale 1:62,500.
- Kruckenber, S.C., D.L. Whitney, C. Teyssier, C.M. Fanning, and W.J. Dunlap, W.J. 2008. Paleocene-Eocene migmatite crystallization, extension, and exhumation in the hinterland of the northern Cordillera: Okanogan dome, Washington, USA. *Geological Society of America Bulletin* 120: 912 – 929.
- Lehman, T.M. 1986. Late Cretaceous sedimentation in Trans-Pecos Texas, in Pause, P.H., and R.G. Spears, eds., *Geology of the Big Bend area and Solitario dome, Texas*. Midland, Texas: West Texas Geological Society 1986 Field Trip Guidebook, Publication 86-82: 105 – 110.
- Lehman, T.M. 1991. Sedimentation and tectonism in the Laramide Tornillo Basin of West Texas. *Sedimentary Geology* 75: 9 – 28.
- Lehman, T.M. 2002a. A review of Late Cretaceous sedimentation in the Big Bend region, in White, J.C., ed. *The geology of Big Bend National Park: What have we learned since Maxwell and others (1967)? Field Trip Guide*: Geological Society of America South-Central Meeting: p. 15 - 18.

- Lehman, T.M. 2002b. A view of the Tornillo Group, in White, J.C., ed. *The geology of Big Bend National Park: What have we learned since Maxwell and others (1967)? Field Trip Guide*: Geological Society of America South-Central Meeting: p. 54-58.
- Lehman, T.M. 2004. Mapping of Upper Cretaceous and Paleogene strata in Big Bend National Park, Texas. *Geological Society of America Abstracts with Programs* 36: 129.
- Levinson, A.A. 1962. Beryllium-fluorine mineralization at Aguachile Mountain, Coahuila, Mexico. *American Mineralogist* 47: 67 – 74.
- Lowell, J.D. 1983. Foreland deformation, in Lowell, J.D., and R. Gries, eds. *Rocky Mountain foreland basins and uplifts*. Denver Colorado: Rocky Mountain Association of Geologists: 1 – 8.
- MacLeod, W. 2003. *Big Bend vistas*. Alpine, Texas: Texas Geological Press.
- Maler, M.O. 1990. Dead Horse graben: A West Texas accommodation zone. *Tectonics* 9: 1357 – 1368.
- Marshak, S. 2008. *Earth, portrait of a planet, third edition*. New York, New York: W.H. Norton & Co.
- Martin, D.M. 2007. *The structural evolution of the McKinney Hill laccolith, Big Bend National Park, Texas* [Master's thesis]. Lubbock, Texas: Texas Tech University.
- Maxson, J., and B. Tikoff. 1996. Hit-and-run collision model for the Laramide orogeny, western United States. *Geology* 24: 968 – 972.
- Maxwell, R.A., J.T. Lonsdale, R.T. Hazzard, and J.A. Wilson. 1967. *Geology of Big Bend National Park, Brewster County, Texas*. Austin, Texas: Bureau of Economic Geology Publication 6711, map scale 1: 62,500.
- McAnulty, W.N., C.R. Sewell, D.R. Atkinson, and J.M. Rasberry. 1963. Aguachile beryllium-bearing fluorspar district, Coahuila, Mexico. *Geological Society of America Bulletin* 74: 735 – 744.
- McCormick, C.L., C.I. Smith, and C.D. Henry. 1996. Cretaceous stratigraphy, in Henry, C.D., and W.R. Muehlberger, eds. *Geology of the Solitario dome, Trans-Pecos Texas: Paleozoic, Mesozoic, and Cenozoic sedimentation, tectonism, and magmatism*. Austin, Texas: Bureau of Economic Geology Report of Investigations No. 240: 30 - 46.
- Miller, D.M., T.H. Nilsen, and W.L. Bilodeau. 1992. Late Cretaceous to early Eocene geologic evolution of the U.S. Cordillera, in Burchfiel, B.C., P.W. Lipman, and M.L. Zoback, eds. *The Cordilleran orogen: Conterminous U.S.* Boulder Colorado: Geological Society of America, The Geology of North America G-3: 205 – 260.

- Mitra, S. and V.S. Mount. 1998. Foreland basement-involved structures. *American Association of Petroleum Geologists Bulletin* 82: 70 – 109.
- Miggins, D.P., M. Ren, E. Anthony, A. Iriondo, and J. Wooden. 2006. New constraints on the timing of volcanism and associated intrusive rocks in Big Bend National Park using $^{40}\text{Ar}/^{39}\text{Ar}$ and U-Pb SHRIMP geochronology. *Geological Society of America Abstracts with Programs* 36: 128.
- Molina-Garza, R.S. and A. Iriondo. 2007. The Mojave-Sonora megashear: The hypothesis, the controversy, and the current state of knowledge, in Alaniz-Alvarez, S.Á. and Nieto-Samaniego, Á.F., eds. *Geology of México: Celebrating the Centenary of the Geological Society of México*. Boulder, Colorado: Geological Society of America Special Paper 442: 233-259.
- Moon, C.G. 1953. Geology of Agua Fria Quadrangle, Brewster County, Texas. *Geological Society of America Bulletin* 64: 151 – 196.
- Morgan, L.A., W.C. Shanks, and W.C. McIntosh. 2006. Early Oligocene flare up in Big Bend National Park, Texas: Contemporaneous activity at Dagger Flats intrusive sill complex and Pine Canyon caldera. *Geological Society of America Abstracts with Programs* 38: 34.
- Moustafa, A.R., 1988, *Structural geology of Sierra del Carmen, Trans-Pecos Texas*. Austin, Texas: Bureau of Economic Geology Geologic Quadrangle Map No. 54. map scale 1:48,000.
- Muehlberger, W.R. 1980. The Texas lineament revisited, in Dickerson, P.W. and J.M. Hoffer, eds., *Trans-Pecos region, southeastern New Mexico and West Texas*. Socorro, New Mexico: New Mexico Geological Society 31st Field Conference Guidebook: 113 – 121.
- Muehlberger, W.R. 1989. Summary of the structural geology of Big Bend National Park and vicinity, in Muehlberger, W.R. and P.W. Dickerson, eds. *Structure and Stratigraphy of Trans-Pecos Texas: Field Trip Guidebook T317, 28th International Geological Congress*. Washington D.C.: American Geophysical Union: 35 - 54.
- Muehlberger, W.R. 1993. *Tectonic map of North America*. Tulsa, Oklahoma: American Association of Petroleum Geologists, map scale 1:5,000,000.
- Muehlberger, W.R., R.C. Belcher, and L.K. Goetz. 1978. Quaternary faulting in Trans-Pecos Texas. *Geology* 6: 337 – 340.
- Muehlberger, W.R. and P.W. Dickerson. 1989. A tectonic history of Trans-Pecos Texas, in Muehlberger, W.R., and P.W. Dickerson, eds. *Structure and Stratigraphy of Trans-Pecos Texas: Field Trip Guidebook T317, 28th International Geological Congress*. Washington D.C.: American Geophysical Union: 35 - 54.

- Muehlberger, W.R. and R.W. Merritt, 1985. Notes on pull-apart grabens near Boquillas Canyon, Big Bend National Park, in Dickerson, P.W. and W.R. Muehlberger, eds. *Structure and tectonics of Trans-Pecos Texas*. Midland, Texas: West Texas Geological Society Field Conference, Publication 85-81: 169 - 171.
- Oldow, J.S., A.W. Bally, H.G. Avé Lallemant, and W.P. Leeman. 1989. Phanerozoic evolution of the North American Cordillera; United States and Canada, in Bally, A.W. and A.R. Palmer, eds. *The Geology of North America – An overview*. Boulder, Colorado: Geological Society of America, The Geology of North America A: 139 – 232.
- Oldow, J.S. 1992. Late Cenozoic displacement partitioning in the northwestern Great Basin, in Craig, S.D., ed. *Structure, tectonics, and mineralization of the Walker Lane: Walker Lane Symposium*. Reno, Nevada: Geological Society of Nevada: 17 – 52.
- Oldow, J.S. 2003. Active transtensional boundary zone between the western Great Basin and Sierra Nevada block, western U.S. Cordillera. *Geology* 31: 1033 – 1036.
- Oldow, J.S., C.L.V. Aiken, J.L. Hare, J.F. Ferguson, and R.F. Hardyman. 2001. Active displacement transfer and differential block motion within the central Walker Lane, western Great Basin. *Geology* 29: 19 – 22.
- Oldow, J.S., A.W. Bally, and H.G. Avé Lallemant. 1990. Transpression, orogenic float, and lithospheric balance. *Geology* 18: 991 – 994.
- Oldow, J.S., G. Kohler, and R.A. Donelick. 1994. Late Cenozoic displacement transfer in the Walker Lane strike-slip belt. *Geology* 22: 637 – 640.
- Page, W.R., K.J. Turner, and R.G. Bohannon. 2008. Tectonic history of Big Bend National Park in Gray, J.E. and W.R. Page, eds. *Geological, geochemical, and geophysical studies by the U.S. Geological Survey in Big Bend National Park, Texas*. Reston, Virginia: U.S. Geological Survey Circular 1327: 3 – 13.
- Poth, S. 1979. *Structural transition between the Santiago and Del Carmen Mountains in northern Big Bend National Park, Texas* [M.A. thesis]. Austin, Texas: University of Texas at Austin. map scale 1:12,000.
- Proffett, J.M., Jr. 1977. Cenozoic geology of the Yerington district, Nevada, and implications for the nature and origin of Basin and Range faulting. *Geological Society of America Bulletin* 88: 247 – 266.
- Proffett, J.M., Jr. and J.H. Dilles. 1984. *Geologic map of the Yerington District, Nevada*. Reno, Nevada: Nevada Bureau of Mines and Geology Map 77. map scale 1:24,000.
- Price, J.G. and C.D. Henry. 1984. Stress orientations during Oligocene volcanism in Trans-Pecos Texas: Timing the transition from Laramide compression to Basin and Range tension. *Geology* 12: 238 – 241.

- Price, J.G. and C.D. Henry. 1985. Summary of Tertiary stress orientations and tectonic history of Trans-Pecos Texas in Dickerson, P.W. and W.R. Muehlberger, eds. *Structure and tectonics of Trans-Pecos Texas*. Midland, Texas: West Texas Geological Society Field Conference, Publication 85-81: 149 – 151.
- Price, J.G. and C.D. Henry. 1988. Dikes in Big Bend National Park; Petrologic and tectonic significance, in O.T. Hayward, ed. *Centennial Field Guide v. 4, South-Central Section of the Geological Society of America*. Boulder, Colorado: Geological Society of America: 435 – 440.
- Price, J.G., C.D. Henry, A.R. Standen, and J.S. Posey. 1985. *Origin of silver-copper-lead deposits in red-bed sequences of Trans-Pecos Texas: Tertiary mineralization in Precambrian, Permian, and Cretaceous sandstones*. Austin, Texas: Bureau of Economic Geology Report of Investigations No. 145.
- Price, J.G., C.D. Henry, and A.R. Standen. 1989. Mineral resources of Trans-Pecos, Texas, in Muehlberger, W.R., and P.W. Dickerson, eds. *Structure and Stratigraphy of Trans-Pecos Texas: Field Trip Guidebook T317, 28th International Geological Congress*. Washington D.C.: American Geophysical Union: 97 - 112.
- Prothro, L.B. 1989. *Structural analysis of the Willoughby thrust fault, Indio Mountains, Hudspeth County, Texas* [Master's thesis]. Canyon, Texas: West Texas State University. map scale 1:12,000.
- Reynolds, S.J., J.K. Johnson, M.M. Kelly, P.J. Morin, and C.M. Carter. 2008. *Exploring Geology*. New York, New York: McGraw-Hill Higher Education.
- Robison, B.A. 1983. Low-angle normal faulting, Marys River Valley, Nevada, in Bally, A.W., ed. *Seismic expression of Structural Styles, A picture and work atlas, Volume 2*. Tulsa, Oklahoma: American Association of Petroleum Geologists Studies in Geology #16, 2.2.2-12 – 2.2.2 - 16.
- Rohrbaugh, R. and C.L. Andronicos. 2000. Tectonic history of the Indio Mountains, West Texas. *Geological Society of America Abstracts with Programs* 32: 232.
- Satterfield, J.I. and J.E. Dyess. 2007. Polyphase folds and faults in a wrench fault zone, northern Big Bend National Park. *West Texas Geological Society Bulletin* 46: 8 – 19.
- Satterfield, J.I., C. Poppeliers, J. Dyess, R. Sonntag, and A.G. Garcia. 2007. Polyphase folds and faults in a wrench fault zone, northern Big Bend National Park, Texas. *Geological Society of America Abstracts with Programs* 39: 634.
- Satterfield, J.I., C.A. Barker, R.L. Nielson, R. Sonntag, and H.F. Schreiner III. 2008. Folding on the flanks of the southernmost Laramide uplift, Big Bend region, Texas. *Geological Society of America Abstracts with Programs* 40.

- Scott, R.B., L.W. Snee, W.R. Page, C.A. Finn, B. Drenth, and E.D. Anderson, E.D. 2004. Oligocene Rosillos Mountains Laccolith, Big Bend National Park. *Geological Society of America Abstracts with Programs* 36: 128.
- Sharpe, R.D. 1980. *Development of the mercury mining industry: Trans-Pecos Texas*. Austin, Texas: Bureau of Economic Geology Mineral Resource Circular No. 64.
- Silver, L.T. and T.H. Anderson. 1974. Possible left-lateral early to middle Mesozoic disruption of the southwestern North America craton margin. *Geological Society of America Abstracts with Programs* 6: p. 955 – 956.
- Smith, C.I., 1970. Lower Cretaceous stratigraphy, northern Coahuila, Mexico. Austin, Texas: Bureau of Economic Geology Report of Investigations No. 65.
- Sonntag, R.C., and J.I. Satterfield, Detailed mapping of easternmost Laramide structures, southeastern Marathon uplift, West Texas. *112th Annual Meeting of the Texas Academy of Science Program and Abstracts*, in review.
- Stenzel, W.K. 1986. 1965 / 1972 road logs, in Pause, P.H. and R.G. Spears, eds. *Geology of the Big Bend area and Solitario dome, Texas*. Midland, Texas: West Texas Geological Society 1986 Field Trip Guidebook, Publication 86-82: 167 - 277.
- Stewart, J.H. 1980. *Geology of Nevada: A discussion to accompany the Geologic Map of Nevada*. Reno, Nevada: Nevada Bureau of Mines and Geology Special Publication 4.
- Stewart, J.H. 1988. Tectonics of the Walker Lane belt, western Great Basin: Mesozoic and Cenozoic deformation in a zone of shear, in Ernst, W.G., ed., *Metamorphism and crustal evolution of the western United States*. Englewood Cliffs, New Jersey: Prentice Hall, Rubey Volume VII: 683 – 713.
- Stewart, J.H. 1998. Regional characteristics, tilt domains, and extensional history of the late Cenozoic Basin and Range province, western North America, in Faulds, J.E. and J.H. Stewart, eds. *Accommodation zones and transfer zones: The regional segmentation of the Basin and Range province*. Boulder, Colorado: Geological Society of America Special Paper 323: 47 – 74.
- Stewart, J.H. and J.C. Crowell. 1989. Strike-slip tectonics in the Cordilleran region, western United States, in Burchfiel, B.C., P.W. Lipman, and M.L. Zoback, eds. *The Cordilleran orogen: Conterminous U.S.* Boulder Colorado, Geological Society of America, The Geology of North America G-3: 609 - 628.
- Stevens, J.B. 1994. Stop 8, Dugout Wells, in Laroche, T.M. and J.J. Viveiros, eds. *Structure and tectonics of the Big Bend area and southern Permian basin, Texas*. Midland, Texas: West Texas Geological Society 1994 Field Trip Guidebook, Publication 94 – 95: 87.

- Stevens, J.B. and M.S. Stevens. 1985. Basin and Range deformation and depositional timing, Trans-Pecos Texas, in Dickerson, P.W. and W.R. Muehlberger, eds. *Structure and tectonics of Trans-Pecos Texas*. Midland, Texas: West Texas Geological Society Field Conference, Publication 85-81: 157 – 164.
- Stevens, J.B. and M.S. Stevens. 1989a. Road logs, field trip to Big Bend region, Trans-Pecos, Texas, in Dickerson, P.W., M.S. Stevens, and J.B. Stevens, eds. *Geology of the Big Bend and Trans-Pecos Region, Fieldtrip Guidebook of the South Texas Geological Society*. Corpus Christi, Texas: South Texas Geological Society: 1 – 72.
- Stevens, J.B., and Stevens, M.S., 1989b, Stratigraphy and major structural-tectonic events along and near the Rio Grande, Trans-Pecos Texas and adjacent Chihuahua and Coahuila, Mexico, in Dickerson, P.W., M.S. Stevens, and J.B. Stevens, eds. *Geology of the Big Bend and Trans-Pecos Region, Fieldtrip Guidebook of the South Texas Geological Society*. Corpus Christi, Texas: South Texas Geological Society: 56 – 94.
- St. John, B.E. 1966. *Geology of the Black Gap area, Brewster County, Texas*. Austin, Texas: Bureau of Economic Geology Geologic Quadrangle Map No. 30. map scale 1:62,500.
- Surpless, B. 2007. Structural complexity within the Black Gap syncline, West Texas: *Geological Society of America Abstracts with Programs* 39: 228.
- Tauvers, P.R. and W.R. Muehlberger. 1988. Persimmon Gap in Big Bend National Park, Texas; Ouachita facies and Cretaceous cover deformed in a Laramide overthrust, in O.T. Hayward, ed. *Centennial Field Guide v. 4, South-Central Section of the Geological Society of America*. Boulder, Colorado: Geological Society of America, p. 435 – 440.
- Toelle, B.E. 1981. *Structural geology of the Persimmon Gap area of Big Bend National Park, Brewster County, Texas, based on remote sensing and field methods* [M.S. Thesis]. Nacogdoches, Texas: Stephen F. Austin State University. map scale 1:12,000.
- Tetreault, J., C.H. Jones, E. Erslev, S. Larson, M. Hudson, and S. Holdaway. 2008. Paleomagnetic and structural evidence for oblique slip in a fault-related fold, Grayback monocline, Colorado. *Geological Society of America Bulletin* 120: 877 – 892.
- Tikoff, B. and J. Maxson. 2001. Lithospheric buckling of the Laramide foreland during Late Cretaceous and Paleogene, western United States. *Rocky Mountain Geology* 36: 13 – 35.
- Twiss, P.C. 1959. *Geologic map of Van Horn Mountains, Texas*. Austin, Texas: Bureau of Economic Geology Quadrangle Map No. 23. map scale 1:48,000.
- U.S. Geological Survey and Nevada Bureau of Mines and Geology. 2006. Quaternary fault and fold database for the United States. <http://earthquakes.usgs.gov/regional/qfaults/> (accessed July 19, 2008).

- Wallace, R.E. 1978. Geometry and rates of change of fault-generated range fronts, north-central Nevada. *Journal of Research, U.S. Geological Survey* 6: 637 – 650.
- Wallace, R.E. 1984. Patterns and timing of Quaternary faulting in the Great Basin province and relation to some regional tectonic features. *Journal of Geophysical Research* 89: 5763-5769.
- Wernicke, B., 1992. Cenozoic extensional tectonics of the U.S. Cordillera, in Burchfiel, B.C., P.W. Lipman, and M.L. Zoback, eds. *The Cordilleran orogen: Conterminous U.S.* Boulder Colorado: Geological Society of America, *The Geology of North America*, G-3: 553 - 581.
- Whitford-Stark, J.L. 1989. A review and new interpretation of structural deformation of the Paleozoic sequence at Persimmon Gap, Big Bend National Park, Texas, in Dickerson, P.W., M.S. Stevens, and J.B. Stevens, eds. *Geology of the Big Bend and Trans-Pecos Region, Fieldtrip Guidebook of the South Texas Geological Society*. Corpus Christi, Texas: South Texas Geological Society: 176 – 194.
- Wilcox, R.E., T.P. Harding, and D.R. Seely. 1973. Basic wrench tectonics. *American Association of Petroleum Geologists Bulletin* 57: 74 – 96.
- Wilson, J.A. 1970. Vertebrate biostratigraphy of Trans-Pecos Texas, in Seewald, K. and D. Sundeen, eds. *The geologic framework of the Chihuahua tectonic belt*. Midland, Texas: West Texas Geological Society, p. 158 – 166.
- Yates, R.G., and G.A. Thompson. 1959. *Geology and quicksilver deposits of the Terlingua district, Texas*. U.S. Geological Survey Professional Paper 312.
- Zimmerman, N.M. 2005. *Host rock fracture analysis: Applying the deformation mechanics associated with shallow igneous intrusion to the fracture bridging theory, McKinney Hills laccolith, Big Bend National Park, USA* [Master's thesis]. Lubbock, Texas: Texas Tech University.
- Zoback, M.L. 1989. State of stress and modern deformation of the northern Basin and Range province. *Journal of Geophysical Research* 94: 7105 – 7128.
- Zoback, M.L., R.E. Anderson, and G.A. Thompson. 1981. Cainozoic evolution of the state of stress and style of tectonism of the Basin and Range province of the western United States. *Philosophical Transactions of the Royal Society of London A* 300: 407 – 434.
- Zoback, M.L. and G.A. Thompson. 1978. Basin and Range rifting in northern Nevada: Clues from a mid-Miocene rift and its subsequent offsets. *Geology* 6: 111- 116.

ACKNOWLEDGEMENTS

Field work in the Dog Canyon-Dagger Mountain area was supported by Carr Research, President's Circle, and Research Enhancement grants from Angelo State University. Research permits from Big Bend National Park and the Black Gap Wildlife Management Area allowed access to this area. Lon Slaughter allowed access to his ranch and encouraged our mapping in the southeastern Marathon uplift. Christian Poppeliers, Henry Schreiner, Ryan Sonntag, and Alexander Stewart reviewed an earlier version of the text and figures. Suggestions by two anonymous reviewers also significantly improved the paper.

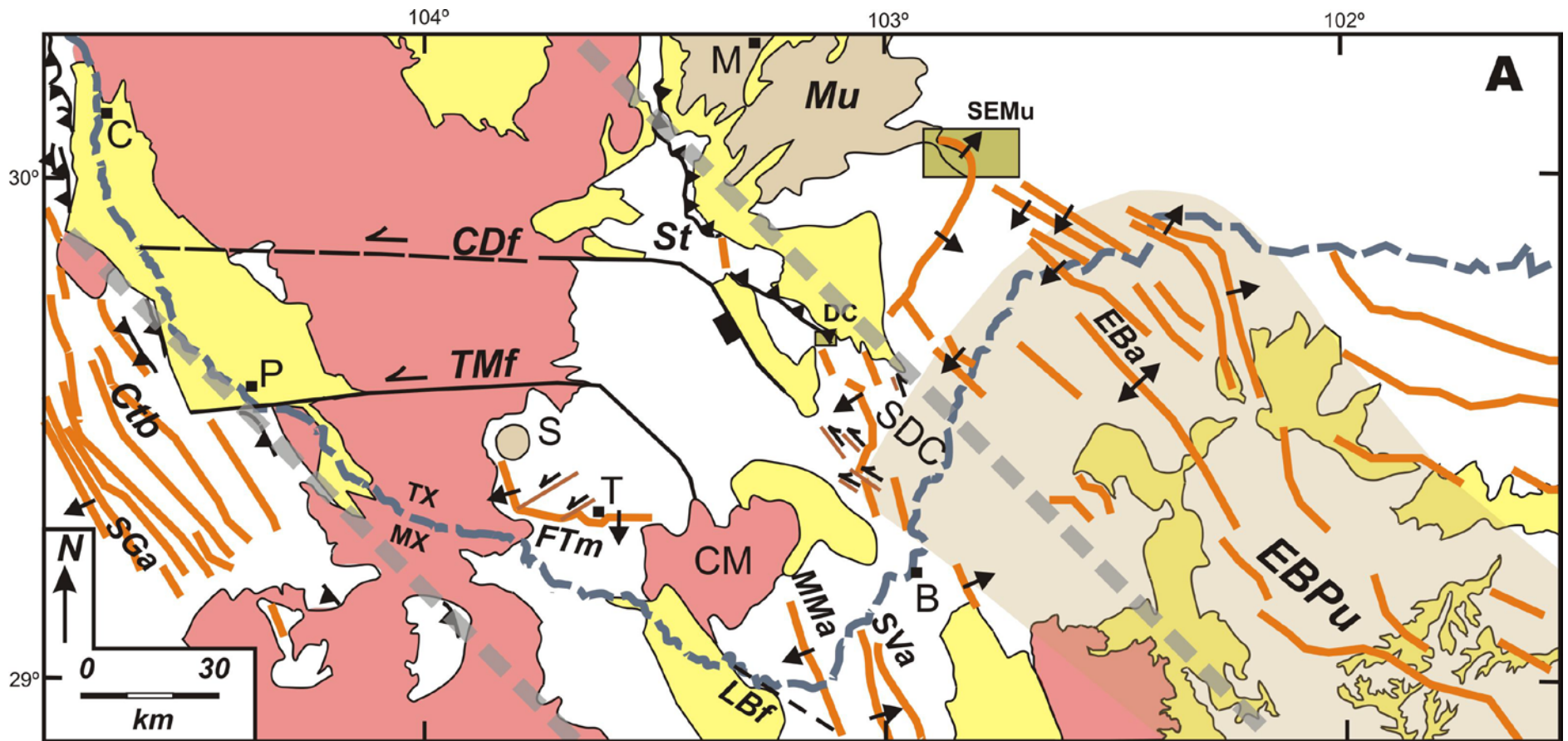
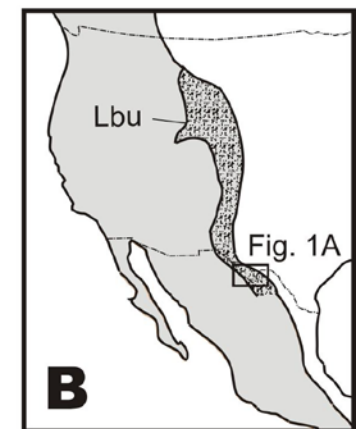


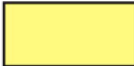




Figure 1. Compilation of Laramide structures in the Big Bend Region.



A) Named structures are discussed in text. See key on separate page for key to abbreviations, symbols, and colors. Sources of data: Muehlberger (1980), Muehlberger and Dickerson (1989), Moustafa (1988), Henry and others (1985), St. John (1966), Charleston (1981), Smith (1970), Carpenter (1997), and Dickerson (1985).






B) Location map showing Cordilleran orogen (gray shades). Lbu- area of Laramide basement uplifts in United States. Modified from English and Johnston (2004)



KEY TO COMPILATION OF LARAMIDE STRUCTURES

	Quaternary and Tertiary sediments
	Tertiary volcanic rocks
	Cretaceous - early Eocene sedimentary rocks
	Underlain by shallow Paleozoic rocks (El Burro-Peyotes uplift)
	Paleozoic sedimentary rocks exposed at surface

	Southeastern Marathon uplift map area
	Dog Canyon-Dagger Mountain map area

	Fold; surface trace of axial plane; arrow shows dip direction of steep limb of monocline
	Thrust fault; teeth on upper plate
	High-angle reverse fault; box on upper plate
	Left-lateral strike-slip fault
	Boundary of Texas Lineament of Muehlberger (1980)

Place names

B	Boquillas, Coahuila, at head of Boquillas Canyon
C	Candelaria, TX
CM	Chisos Mountains
M	Marathon, TX
P	Presidio, TX
S	The Solitario
SDC	Sierra del Carmen
T	Terlingua, TX

Named Laramide structures

<i>CDf</i>	Chalk Draw fault
<i>Ctb</i>	Chihuahua tectonic belt
<i>EBa</i>	El Burro anticline
<i>EBPu</i>	El Burro-Peyotes uplift
<i>FTm</i>	Fresno-Terlingua monocline
<i>LBf</i>	La Babia fault
<i>MMa</i>	Mariscal Mountain anticline
<i>Mu</i>	Marathon uplift
<i>SGa</i>	Sierra Grande anticline
<i>St</i>	Santiago thrust
<i>SVa</i>	San Vicente anticline
<i>Tmf</i>	Tascotal Mesa fault

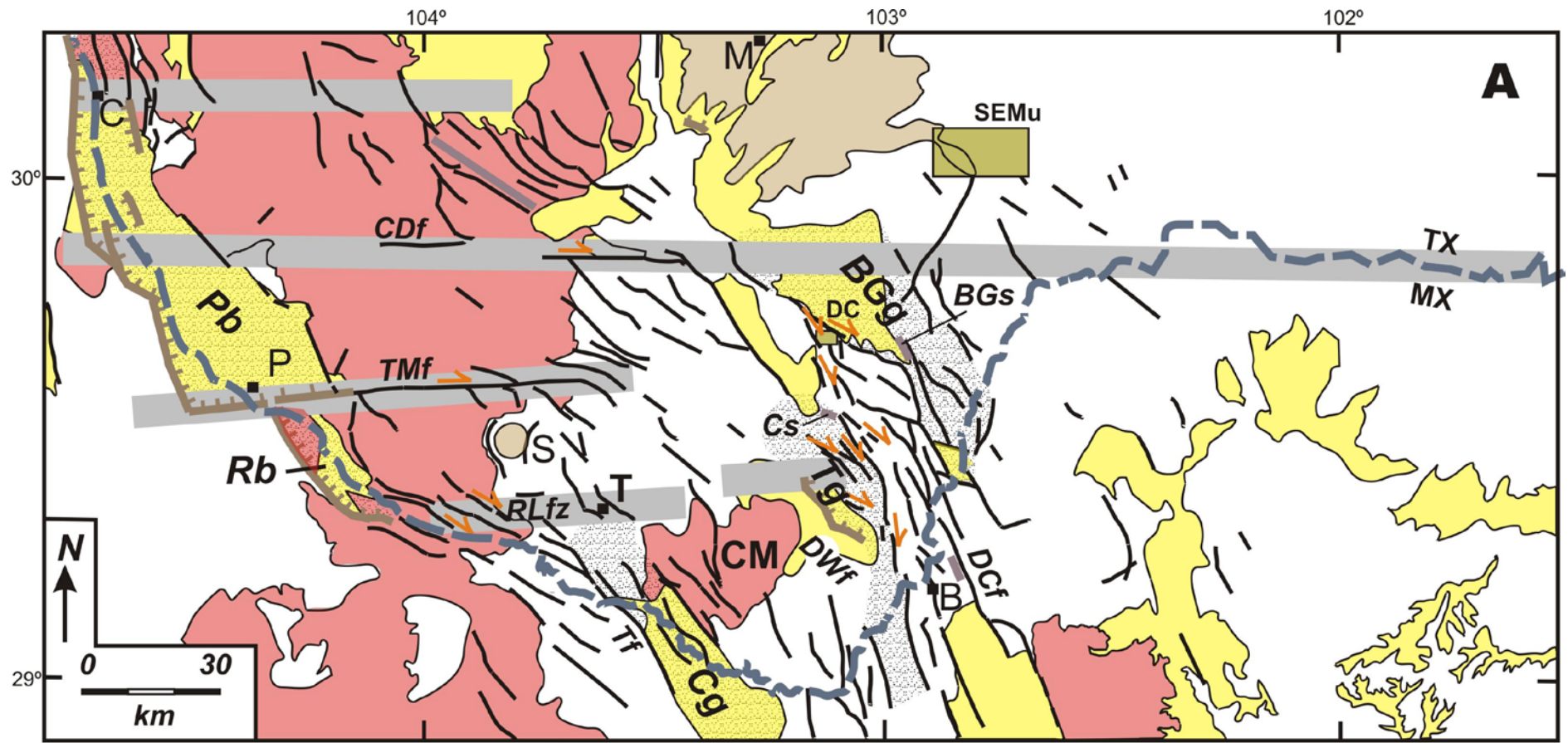
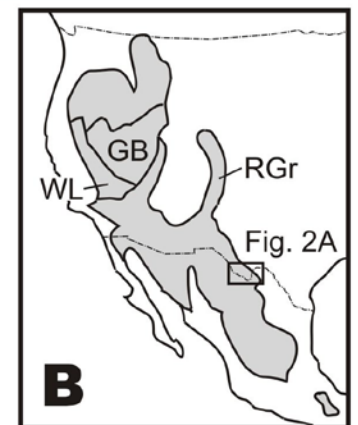



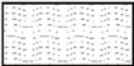



Figure 2. Compilation of Basin and Range structures in the Big Bend Region.



A) Named structures are discussed in text. See key to abbreviations, symbols, and colors on separate page. Modified from Henry and others (1985) to include data from Dickerson (1980), Muehlberger and Dickerson (1989), Moustafa (1988), St. John (1966), Charleston (1981), Smith (1970), Carpenter (1997), Collins (1994), Charleston (1980), Carpenter (1997), Smith (1970), Goldich and Seward (1948), and Dickerson (1985).






B) Location map showing Basin and Range province (gray shade). GB- Great Basin, RGr- Rio Grande rift, WL- Walker Lane. Map modified from Stewart (1998).



KEY TO COMPILATION OF BASIN AND RANGE STRUCTURES

	Quaternary and Tertiary sediments
	Named graben
	Tertiary volcanic rocks
	Cretaceous rocks
	Paleozoic rocks exposed at surface

	SEMu Southeastern Marathon uplift map area
	DC Dog Canyon-Dagger Mountain map area

	Fold; surface trace of axial plane
	Normal fault
	documented Quaternary normal fault
	Right-lateral strike-slip fault
	Structural zone of Dickerson (1980) and Stevens and Stevens (1989)

Place names

B	Boquillas, Coahuila, at head of Boquillas Canyon
C	Candelaria, TX
CM	Chisos Mountains
M	Marathon, TX
P	Presidio, TX
S	The Solitario
SDC	Sierra del Carmen
T	Terlingua, TX

Named grabens

<i>BGg</i>	Black Gap graben
<i>Cg</i>	Castelon graben
<i>Pb</i>	Presidio bolson
<i>Rb</i>	Redford bolson
<i>Tg</i>	Tornillo graben

Named structures

<i>BGs</i>	Black Gap syncline
<i>Cs</i>	Canoe syncline
<i>CDf</i>	Chalk Draw fault
<i>DCf</i>	Del Carmen fault
<i>DWf</i>	Dugout Wells fault
<i>RLfz</i>	Redford-Lajitas fault zone
<i>TMf</i>	Tascotal Mesa fault
<i>Tf</i>	Terlingua fault



Figure 3. Laramide overturned syncline cross-cut by Dog Canyon, Sierra del Carmen, Big Bend National Park. Figures 1 and 2 locate the Dog Canyon area. View is to the north.

A) Panorama shows a Laramide fold best defined by thick beds within cliff-forming Santa Elena Limestone and the contact between Santa Elena limestone and overlying slope-forming Del Rio Clay on north side of canyon define fold. Fold trends north-northeast. Panorama by R.A. Ashmore is a composite of 78 images.

B) Line drawing of panorama shows geologic interpretation of panorama area. Geologic map units, all Cretaceous age, oldest listed first: Kgr- Glen Rose Limestone, Kdc- Del Carmen Limestone, Ksp- Sue Peaks Formation (defined by trough on north side of Dog Canyon), Kse- Santa Elena Limestone, Kdr- Del Rio Clay, Kbu- Buda Limestone. Other symbols: thin line containing double dot pattern- surface trace of axial plane of Laramide (D₂) overturned syncline, heavy black line- Laramide (D₂) thrust fault, teeth on upper plate. The surface trace of the axial plane is the intersection of the earth's surface with the axial plane, the imaginary plane that bisects the overturned syncline. The well-exposed thrust cross-cuts the overturned syncline (see geologic map in Satterfield and Dyess 2007), but is not easily visible from this vantage point

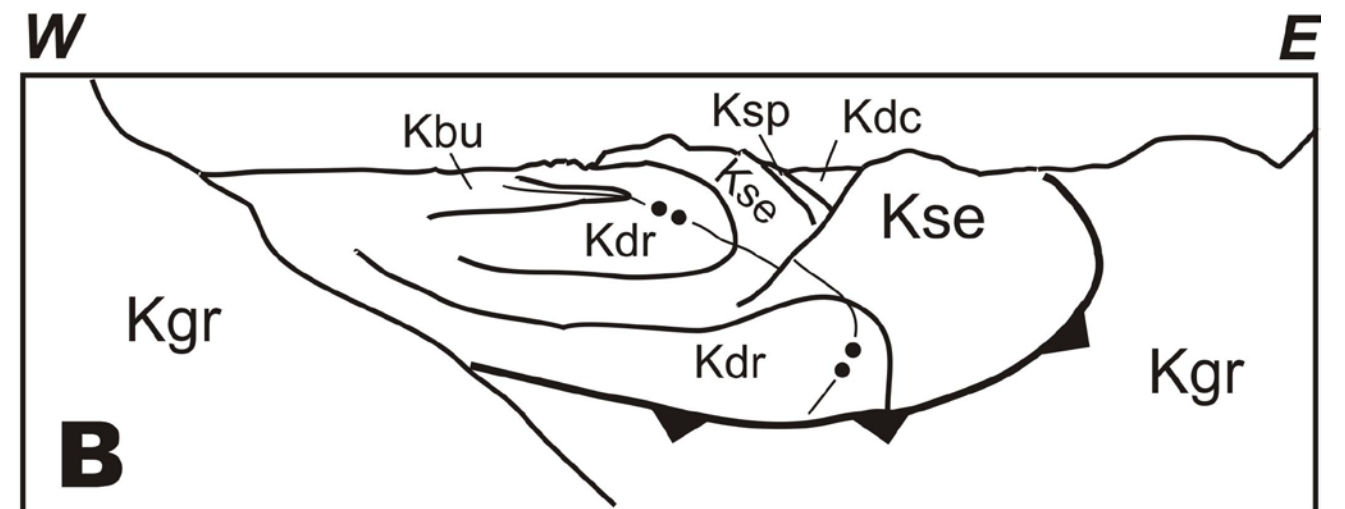




Figure 4. Northwest-trending fault surface in Boquillas Canyon displaying low-angle slickenlines diagnostic of strike-slip component of offset. Fault juxtaposes relatively thin-bedded limestone on right from wall of very thick-bedded limestone on the left. Slickenlines (some identified with arrows) on calcite-mineralized fault surface are plunging to the right. Photograph by J.I. Satterfield.



A

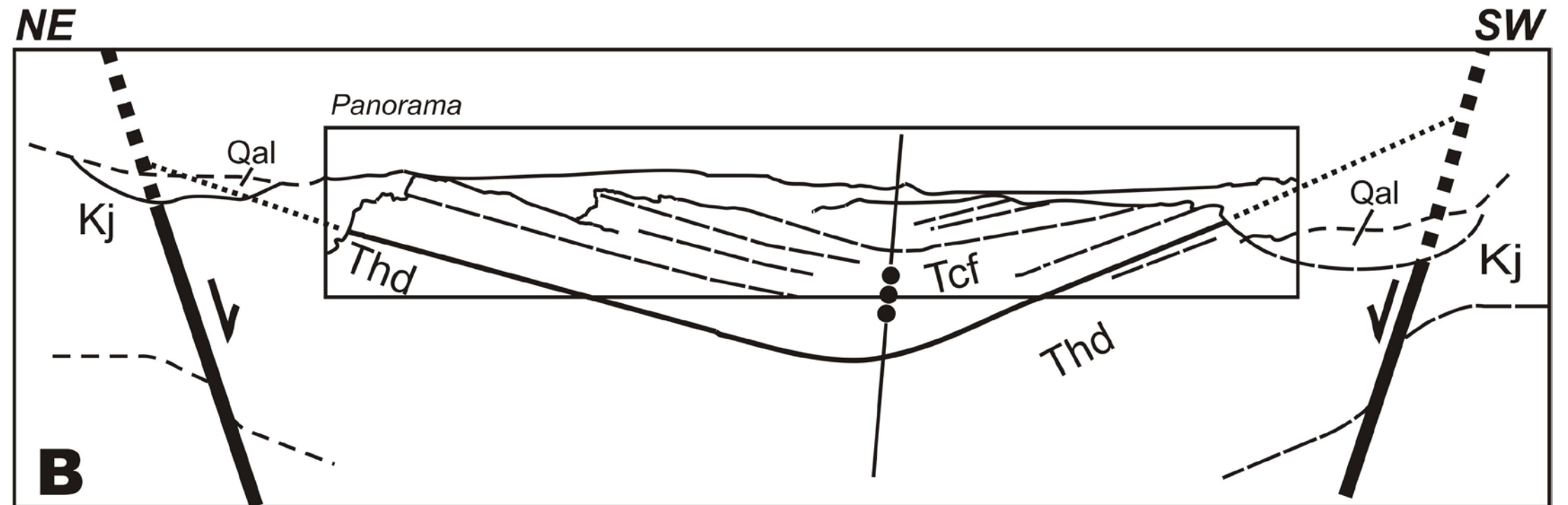


Figure 5. Canoe syncline within Tornillo graben, Big Bend National Park. Canoe syncline is located on Figure 2. View is to the southeast, down the shallowly plunging fold axis of the syncline. Sierra del Carmen is on northeast horizon. Figure 67 in Maxwell et al. (1967) is a panorama of this view taken from the same vantage point.

A) Panorama shows a Basin and Range fold defined by beds within the Big Yellow Sandstone of the lowermost Canoe Formation (the Formation is named after this fold). Fold trends northwest. Panorama by R.A. Ashmore is a composite of nine images.
 B) Line drawing of panorama and surrounding area shows geologic interpretation. Geologic map units, oldest listed first: Kj- Cretaceous Javelina Formation, Thh- 53 - 51 Ma (Tertiary) Hannold Hill Formation, Tcf- 51 - 47 Ma (Tertiary) Canoe Formation, Qal- Quaternary stream deposits (numerical ages of Formations from Lehman 1991). Other symbols: thin line containing triple-dot pattern- axial plane of Basin and Range (D₃) syncline, heavy black lines- Basin and Range normal faults bounding a narrow graben within the Tornillo graben. The position of the Canoe syncline within the axis of a narrow Basin and Range graben, its post-51 Ma timing, and its northwest-trending axial plane orientation document that the Canoe syncline formed during Basin and Range extension.